

DEPENDENCE OF THE HELIUM II FILM  
TRANSFER RATE ON PRESSURE HEAD,  
FILM HEIGHT, AND SUBSTRATE

Thesis for the Degree of Ph. D.  
MICHIGAN STATE UNIVERSITY  
CARL JAMES DUTHLER  
1970

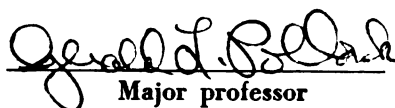


This is to certify that the  
thesis entitled  
Dependence of the Helium II Film Transfer Rate  
on Pressure Head, Film Height, and Substrate  
presented by

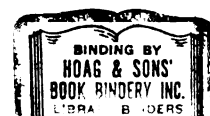
Carl James Duthler

has been accepted towards fulfillment  
of the requirements for

Ph.D. degree in Physics

  
Major professor

Date August 28, 1970



## ABSTRACT

### DEPENDENCE OF THE HELIUM II FILM TRANSFER RATE ON PRESSURE HEAD, FILM HEIGHT, AND SUBSTRATE

By

Carl James Duthler

Helium film transfer rates,  $\sigma$ , have been measured as a function of level difference,  $z$ , and height,  $h$  to the beaker rim, for filling clean glass and neon coated beakers. Measured transfer rates as a function of level difference or pressure head are described by:  
 $\sigma(z) = 1/[A - B \ln z(\text{cm})]$ . For  $T = 1.65 \text{ K}$  and  $h = 7 \text{ cm}$ , the values  $A = (1.80 \pm 0.09) \times 10^4 \text{ sec/cm}^2$  and  $B = (8.9 \pm 1.9) \times 10^2 \text{ sec/cm}^2$  are found. For  $T = 1.28 \text{ K}$  and  $h = 7 \text{ cm}$ , the values  $A = (1.35 \pm 0.02) \times 10^4 \text{ sec/cm}^2$  and  $B = (8.4 \pm 1.4) \times 10^2 \text{ sec/cm}^2$  are found. The dependence of the transfer rate on height is:  
 $\sigma(h) = 10(\rho_g/\rho)h^{-(0.26 \pm 0.05)} \times 10^5 \text{ cm}^3/\text{sec-cm}$ . These observations give the dependence,  $P_g = \exp[f(h,T)/v_g]$ , of the frictional pressure,  $P_g$  which opposes the flow, on superfluid velocity,  $v_g$ . The dependence,  $v_c = d^{-1/4}$ , of the critical velocity,  $v_c$ , on film thickness,  $d$ , is also determined from these results.

A 16% decrease is observed in  $\sigma$  going from a clean glass substrate to a neon coated substrate in the same apparatus. This result is in reasonable agreement with the calculated helium film thickness for a neon substrate of  $2.3h^{-1/3} \times 10^{-6} \text{ cm}$ .

DEPENDENCE OF THE HELIUM II FILM TRANSFER RATE ON  
PRESSURE HEAD, FILM HEIGHT, AND SUBSTRATE

By

Carl James Duthler

A THESIS

Submitted to

Michigan State University

in partial fulfillment of the requirements

for the degree of

DOCTOR OF PHILOSOPHY

Department of Physics

1970

667233

**To Karen**

## ACKNOWLEDGEMENTS

This experiment was suggested by Professor G. L. Pollack. I am very much indebted to him for his guidance and encouragement. Thanks are also due to Mr. Garold Fritz and Mr. Charles Leming for many interesting discussions and for their assistance in the laboratory. I would also like to acknowledge my wife, Karen, for her assistance in data acquisition and for typing this thesis. Finally I would like to acknowledge the financial support of the U. S. Atomic Energy Commission.

## TABLE OF CONTENTS

Chapter	Page
I. INTRODUCTION . . . . .	1
A. Properties of Liquid Helium . . . . .	1
B. Properties of the Helium Film . . . . .	3
C. Purpose . . . . .	5
II. THEORETICAL . . . . .	6
A. Theories of the Critical Velocity . . . . .	6
B. Theories of the He Film Thickness . . . . .	12
C. Dynamics of the Film Transfer . . . . .	19
III. EXPERIMENTAL . . . . .	22
A. Clean Glass Substrate Apparatus . . . . .	22
B. Neon Substrate Apparatus . . . . .	29
C. Experimental Procedure . . . . .	38
D. Data Reduction and Experimental Accuracy . . . . .	42
IV. RESULTS AND DISCUSSION . . . . .	47
A. Pressure Head Dependence . . . . .	47
B. Height Dependence . . . . .	54
C. Substrate Dependence . . . . .	60
V. SUMMARY AND CONCLUSIONS . . . . .	66
LIST OF REFERENCES . . . . .	68
 Appendices	
A. COMPUTER PROGRAM FOR DATA REDUCTION . . . . .	72
B. TABULAR TRANSFER RATE DATA . . . . .	78

# LIST OF TABLES

Table		Page
1	Helium film thickness calculated by Schiff.	13
2	Values of the Mie-Lennard-Jones potential parameters $\epsilon$ and $r^*$ and number density $n$ for rare-gas solids and liquid helium.	15
3	Values of the Mie-Lennard-Jones potential parameters $\epsilon$ and $r^*$ for the interaction of helium with rare gas atoms.	15
4	Calculated thickness of He film on rare-gas solid substrate.	16
A1	Fortran listing of the computer program, Sigma-z, used in the $\sigma(z)$ analysis.	72
A2	Typical input data to computer program for one beaker filling.	75
A3	Computer output for data of Table 2.	76
B1	Measured transfer rate parameters for a clean glass substrate and $T = 1.65$ K.	78
B2	Measured transfer rate parameters for a clean glass substrate and $T = 1.28$ K.	80
B3	Measured transfer rate data for a neon substrate and $T = 1.65$ K.	81



# LIST OF FIGURES

Figure		Page
1	Calculated thickness of the helium film, $d$ with $h = 1$ cm, versus thickness of Ne coating, $\xi$ , on a Xe substrate.	18
2	Schematic drawing of clean glass substrate apparatus.	24
3	Schematic drawing of Ne substrate apparatus.	31
4	Gas handling system for Ne.	37
5	Level difference, $z$ , as a function of time for three beaker fillings at three different heights, $h$ , to the beaker rim.	41
6	Transfer rates, $\sigma(z)$ , from the $z(t)$ curve of a typical run.	44
7	Transfer rate as a function of level difference for the three beaker fillings of Figure 5.	48
8	Log-log plot of the critical transfer rate, $\sigma_c$ with $T = 1.65$ K, versus height, $h$ , to the beaker rim.	56
9	Log-log plot of the critical transfer rate, $\sigma_c$ with $T = 1.65$ K, versus corrected height, $h_{\text{corr}} = h + 1 \frac{1}{2}$ cm.	59
10	Semi-log plot of the critical transfer rate, $\sigma_c$ with $h = 7$ cm and $T = 1.65$ K, versus thickness of Ne coating, $\xi$ .	62

## I. INTRODUCTION

### A. Properties of Liquid Helium

Helium was first liquefied by H. Kamerlingh-Onnes in 1908. Because of weak interatomic forces and large zero point motions, helium, under its saturated vapor, remains liquid even at absolute zero where a pressure of at least 25 atmospheres is necessary for solidification. The normal boiling point of helium is 4.2 K.<sup>1-7</sup>

Early experimenters did not expect anything unusual from the liquid phase of these chemically inert and spherically symmetric atoms. However, there is a phase change in the liquid at 2.172 K, the lambda point. Below the lambda point,  $T_\lambda$ , liquid helium has many unusual properties. The name lambda point comes from the shape of the specific heat curve, which resembles the Greek letter  $\lambda$ , in the vicinity of 2.172 K. Keesom and Keesom<sup>8</sup> discovered this transition in 1936 from measurements of the specific heat. Above  $T_\lambda$  liquid helium behaves as an ordinary liquid and was called helium I by Keesom. Liquid helium below  $T_\lambda$  is called helium II.

Usual methods of measuring the viscosity of He II gave a very low viscosity and different experiments appeared to be contradictory.<sup>1-7</sup> In fact, under certain conditions He II can flow frictionlessly through very narrow channels. Also, the thermal conductivity greatly increased below  $T_\lambda$ . Helium I has a thermal conductivity comparable with room temperature air while He II has an effective thermal

conductivity about 1000 times greater than room temperature copper.

These and other unusual properties of He II are interpreted as a macroscopic manifestation of quantum effects. Because the weakly interacting  $\text{He}^4$  atoms consist of an even number of nucleons and electrons having no net spin, they are somewhat analogous to a non-interacting Bose-Einstein gas.<sup>10</sup> Non-interacting bosons can, below a certain critical temperature, condense into the quantum mechanical ground state with all the atoms in the ground state at absolute zero. The unusual properties of He II are interpreted as a result of the condensation of atoms into the quantum mechanical ground state.

As a result of the theoretical work of Tisza,<sup>9</sup> and of London<sup>10</sup> and Landau,<sup>11</sup> the two fluid model was developed. The two fluid model is a phenomenological model that has been very successful in explaining experimental properties of He II. Helium II is regarded as consisting of two interpenetrating fluids: the normal fluid and the superfluid. Each constituent fluid has its own particle density and to a first approximation its own velocity field. The density of He II,  $\rho$ , is the sum of the normal fluid density,  $\rho_n$ , and the superfluid density,  $\rho_s$ :

$$\rho = \rho_n + \rho_s. \quad (1)$$

The superfluid fraction,  $\rho_s/\rho$ , is associated with the fraction of the atoms in the ground state and is a function of temperature. At  $T = T_\lambda$ , there is only normal fluid, i.e.,  $\rho = \rho_n$ . At  $T = 0$  K, there is only superfluid, i.e.,  $\rho = \rho_s$ .

The hydrodynamics of He II is governed by the two fluid equations of motion:

$$\rho_s \frac{d\vec{v}_s}{dt} = -(\rho_s/\rho) \vec{\nabla} P + \rho_s \vec{\nabla} T \quad (2)$$

and

$$\rho_n d\vec{v}_n/dt = -(\rho_n/\rho)\vec{\nabla}P - \rho_n s\vec{\nabla}T - \eta_n \vec{\nabla} \times (\vec{\nabla} \times \vec{v}_n). \quad (3)$$

Here  $\vec{v}_s$  is the velocity of the superfluid,  $\vec{v}_n$  the velocity of the normal fluid,  $\eta_n$  the coefficient of viscosity of the normal fluid,  $P$  the pressure,  $s$  the entropy per gram, and  $T$  the temperature. We notice that the superfluid equation has no viscosity term. This thesis is concerned with the conditions under which the flow of the superfluid in the helium film remains frictionless.

### B. Properties of the Helium Film

In 1932 Kammerlingh-Onnes noticed that the levels in two containers, connected by the He II film, tended to equalize. This was the first observation of transport in the helium film but the transport was unfortunately interpreted by Kammerlingh-Onnes as being due to evaporation and recondensation. In 1937, Rollin and Simon<sup>12</sup> calculated that evaporation was not able to explain the observed transport. They correctly postulated that mass flow was taking place in a relatively thick, mobile film of helium. As a result, the helium film is often referred to as the "Rollin film".

Physical adsorption is a familiar phenomenon with the usual adsorbates being thin and immobile films, except for small, random atomic motions. The adsorbed He II film is, on the other hand, approximately 80 layers thick and very mobile due to frictionless flow of the superfluid. Also, ordinary films are easily evaporated, but He II films are readily replenished by superfluid flow.

The transport of the He II film provides a convenient means of studying superfluid flow in very small geometries. Typically,

flow into or out of a beaker is measured and the superfluid velocity,  $v_s$ , is related to the transfer rate per unit circumference,  $\sigma$ , by:

$$\sigma = (\rho_s/\rho)v_s d, \quad (4)$$

where  $d$  is the thickness of the film. The factor  $(\rho_s/\rho)$  expresses the fact that only the superfluid component moves while normal fluid, as an ordinary adsorbed film, is immobile.

In 1938, Daunt and Mendelssohn<sup>13</sup> reported the first systematic observations of transfer in the film. In a very thorough and elegant series of experiments they observed that the transport rate depended primarily on the temperature. They also observed that, for constricted beakers, the total transfer rate was proportional to the smallest circumference separating the levels. In addition, the flow was nearly independent of the level difference and the length of the film. These observations led them to postulate that the flow was taking place at a characteristic or critical velocity,  $v_c$ .

Subsequently, Atkins,<sup>14</sup> and independently Esel'son and Lazarev,<sup>15</sup> observed that the transfer rate did depend on the level difference and the height of the beaker rim above the bulk liquid. The dependence of the transfer rate on height arises from the dependence of the film thickness on height which is usually of the form:

$$d = k/h^{1/3}, \quad (5)$$

Here  $d$  is the thickness of the film at a height  $h$  above the bulk liquid and  $k$  is a constant, for a given substrate material, which is equal to  $3.0 \times 10^{-6} \text{ cm}^{4/3}$  for clean glass.<sup>16</sup> However, the actual dependence of  $\sigma$  on  $h$  is less than the dependence of  $d$  on  $h$ , because  $v_c$  is itself a function of  $d$ .

The parameter  $k$  in Equation 5 for the film thickness depends

on the substrate material and results in a dependence of the transfer rate on substrates. Smith and Boorse<sup>17</sup> did a series of careful measurements for several glass and metal substrates. They concluded, however, that the typical 10% background variations in their experiments prevented the resolution of a dependence of  $\sigma$  on substrate for the materials they investigated.

The above general properties of helium are closely related to this thesis. There are several excellent reviews of these and other properties of liquid helium from which more detailed information can be obtained.<sup>1-7</sup>

### C. Purpose

In the present investigation the dependence of the transfer rate on pressure head and film height was examined in more detail. In particular the functional form of these dependences was of interest for comparison with theory. To keep background variations to a minimum, the geometry of the apparatus is kept simple and a very clean, and vibration free, environment is provided for the beaker.

The dependence of the transfer rate on substrate has also been examined for neon coated glass beakers. By coating the beakers with neon, the substrate could be changed from clean glass to neon in the same apparatus. The thickness of the adsorbed helium film on the effective neon substrate was then determined from the transfer rate measurements and compared with the calculated value.

## II. THEORETICAL

### A. Theories of the Critical Velocity

Theories of the critical velocity of He II flowing in narrow channels are examined in this section. A narrow channel is defined to be a channel that is small enough that the normal fluid is immobile. The He II film is considered to be a special case of narrow channels.

The earliest theory of the critical velocity is due to Landau.<sup>11</sup> Although the physical mechanism proposed for the critical velocity is probably not valid, the general approach used by Landau is still used in modern theories. This theory and possible modifications are outlined below.

Landau's theory of He II emphasises the elementary excitations which are associated with the normal fluid rather than the condensation of the superfluid into the Bose-Einstein ground state. Landau separated the elementary excitations into two regions. At low momenta the excitations are phonons, as in a solid, which have a linear dispersion relation:

$$\epsilon(p) = c_1 p. \quad (6)$$

Here  $\epsilon$  is the energy of the phonon with momentum  $p$  and  $c_1$  is a constant equal to the velocity of sound. At higher momenta, Landau proposed another excitation which is unique to this fluid and is called a roton. A roton is a co-operative excitation of many He atoms which is visualized as being similar to a quantized smoke

ring. Rotons have the parabolic dispersion relation:

$$\epsilon(p) = \Delta + (p-p_0)^2/2\mu. \quad (7)$$

Here  $\epsilon$  is the energy of a roton of momentum  $p$ . The minimum roton energy  $\Delta$  occurs at momentum  $p_0$  with  $\Delta/k = 9$  K and  $p_0/\hbar = 2.0 \text{ \AA}^{-1}$ . The effective mass of the roton is one quarter the helium atomic mass, i.e.,  $\mu = m/4$ .<sup>5</sup>

Below the critical velocity, the superfluid flows without dissipation. At the critical velocity dissipation sets in, which Landau regarded as being due to the creation of elementary excitations. If an excitation of energy  $\epsilon$  and momentum  $p$  is created in superfluid, flowing with uniform velocity  $\vec{v}_s$ , the energy change of the superfluid system is:<sup>5</sup>

$$\epsilon(\vec{p}) + \vec{p} \cdot \vec{v}_s < 0. \quad (8)$$

This energy change must be less than zero and the momentum,  $\vec{p}$ , of the excitation is opposite to the superfluid velocity because of the energy and momentum transfer to the wall of the channel.

The critical velocity,  $v_c$ , is the minimum velocity at which this occurs. Solving Equation 8 for  $v_s$ , we get the Landau criterion for the critical velocity:

$$v_c = |\epsilon(p)/p|_{\min} < v_s. \quad (9)$$

For creation of phonons, the resulting critical velocity is, from the dispersion relation,

$$v_{s,ph} = c_1 = \text{velocity of sound} = 2 \times 10^4 \text{ cm/sec.} \quad (10)$$

For creation of rotons, the resulting critical velocity is, from the dispersion relation,

$$v_{s,rot} = \left| \frac{\Delta}{p} + \frac{(p-p_0)^2}{2\mu p} \right|_{\min} = 6 \times 10^3 \text{ cm/sec.} \quad (11)$$



These critical velocities,  $v_{s,ph}$  and  $v_{s,rot}$ , are orders of magnitude larger than the observed critical velocities. The largest observed critical velocity occurs in the He II film and is approximately equal to 50 cm/sec. However, the Landau criterion may still be valid for a higher momentum "excitation". These higher momentum "excitations" are thought to be Feynman-Onsager vortices.

Landau regarded the frictionless character of the superfluid to be a result of curl free behavior in the superfluid, *i.e.*  $\vec{\nabla} \times \vec{v}_s = 0$ . An ideal fluid can, however, have vorticity without curl in the case of multiply connected geometries. Onsager<sup>18</sup> pointed this out in a paper on vorticity where he also mentions, in a footnote, that the circulation should be quantized in multiples of  $h/m$ .

Subsequently, Feynman<sup>19</sup> derived this independently from considerations of the wave function of He II. For He II in uniform motion, at absolute zero the wave function is:

$$\psi = \psi_0 \exp(i\vec{k} \cdot \sum_j \vec{R}_j) \quad (12)$$

where  $\vec{R}_j$  is the position of the  $j^{\text{th}}$  atom and  $\psi_0$  is the wave function for the fluid at rest. The total momentum of the  $N$  helium atoms is  $N\hbar\vec{k}$  where  $\vec{k} = m\vec{v}_s/\hbar$ .

For slightly non-uniform motion the wave function is:

$$\psi = \psi_0 \exp[i(m/\hbar) \sum_j \vec{v}_j(\vec{R}_j) \cdot \vec{R}_j] = \psi_0 \exp[i\phi(\vec{R})]. \quad (13)$$

Feynman points out that the quantum mechanical phase or order parameter,  $\phi(\vec{R})$ , is a slowly varying function of position and time and is the potential for flow.

Using the normalization  $|\psi|^2 = \rho_s$  and taking the quantum mechanical momentum density equal to the superfluid momentum density,

$\sum_j \vec{p}_j = \rho_s \vec{v}_s$ , we get:

$$\vec{v}_s = \vec{J}_s / \rho_s = -(i\hbar/2m\rho_s)(\psi^* \vec{\nabla} \psi - \psi \vec{\nabla} \psi^*) = (\hbar/m) \vec{\nabla} \phi. \quad (14)$$

The condition  $\vec{\nabla} \times \vec{v}_s = 0$  is automatically satisfied. The quantized circulation,  $K$ , is obtained by integrating the velocity around a hole or obstruction in the superfluid:

$$K \equiv \oint \vec{v}_s \cdot d\vec{l} = (\hbar/m) \oint \vec{\nabla} \phi \cdot d\vec{l} = nh/m. \quad (15)$$

Quantization is a result of the requirement that  $\psi$  be single valued. For one revolution around the obstruction the phase,  $\phi$ , must change by  $2\pi$ . Feynman also points out that a physical obstacle is not necessary. All that is needed is a non-superfluid core of atomic dimensions.

We can now apply the Landau criterion to the case of vortices in a channel of diameter  $d$ .<sup>20</sup> In this case we consider the critical velocity to be a result of the production of quantized vortex rings having a diameter approximately equal to the channel diameter.

A free vortex ring has the following energy  $\epsilon$ , and momentum,  $p$ :

$$\epsilon = (\rho K^2 d/4) [\ln(4d/a_0) - \kappa] \quad (16)$$

and

$$p = \pi \rho K d^2/4. \quad (17)$$

Here  $a_0$  is the diameter of the vortex core and  $\kappa$  is a constant of order unity. Applying the Landau criterion we get:

$$v_c = (\epsilon/p)_{\min} = (K/\pi d) [\ln(4d/a_0) - \kappa]. \quad (18)$$

This critical velocity has the correct magnitude but the dependence of  $v_c$  on channel width does not agree with experiment. From the examination of many experimental critical velocities spanning several decades of channel width, Van Alphen *et al.*<sup>21</sup> have proposed

the empirical relation  $v_c \propto d^{-1/4}$ .

Vortex production is, however, considered to be the correct mechanism responsible for the critical velocity. The disagreements with experiment are most likely a result of a lack of knowledge of how the vortices are nucleated and how they interact with the walls of the channel. Some ideas of how the vortices are nucleated are presented below.

Vinen<sup>22</sup> proposed that there is always vorticity present in He II in the form of small pieces of vortex lines. Glaberson and Donnelly<sup>23</sup> extended this idea in their vortex-mill model of nucleation. These pieces of vortex lines are considered to be attached or pinned to irregularities on the channel wall. When the superfluid velocity exceeds the critical velocity, these primordial vortex lines grow, generating new lines at the expense of the kinetic energy of the flow.

Peshkov<sup>24</sup> suggested that the energy to create a vortex comes from the kinetic energy of a certain volume of the superfluid in a short time  $\tau = 10^{-4}$  sec. In this case the length of the volume increases as the channel width decreases resulting in a critical velocity that increases with decreasing channel width. Craig<sup>25</sup> has extended Peshkov's ideas and finds

$$v_c^3 d = B \ln(1 + C/v_c). \quad (19)$$

This functional form does fit the data. However, the constants  $B$  and  $C$  were obtained from experimental data rather than from basic principles.

Langer and Fisher<sup>26</sup> have proposed that vortices can be nucleated by thermal activation. They regard the flowing superfluid as a

metastable state. Thermal fluctuations cause the superfluid density to vanish at isolated points in the superfluid. A vortex can then be created and result in a decrease in the velocity of the superfluid. Langer and Fisher find that the vortices are created at the rate  $f_0 \exp(-\Delta F_B/kT)$  per unit volume in the channel. Here  $\Delta F_B$  is a fundamental fluctuation frequency. The resulting decrease in velocity is  $\Delta v_s = h/ml$  where  $l$  is the length of the channel.

This agrees with the observations by Clow and Reppy<sup>27</sup> of the decay of superfluid persistent currents when the temperature is near the lambda point.

Notarys<sup>28</sup> extended this theory to pressure driven superfluid flow. He derives the frictional pressure along a channel as a function of superfluid velocity and temperature:

$$p = (h/mpVf_0)\exp(-\Delta F_B/kT), \quad (20)$$

where  $V$  is the volume of the channel. Using vortex rings for the dissipation mechanism gives:<sup>28</sup>

$$p = \frac{h}{m} \rho V f_0 \exp\left(-\frac{\beta}{k} \frac{\rho_s}{\rho v_s T}\right), \quad (21)$$

where  $\beta$  is nearly constant.

Notarys finds that this theory agrees with his observations for superfluid flowing through narrow pores with temperatures down to 1 K. In this case there is no "critical" velocity. For any velocity there is a pressure gradient which, however, is very small at low velocities and increases very rapidly at larger velocities.

Although the dynamics of the nucleation of vortices is not known, the rate of production is known from the Josephson frequency. Recent theories have extended Feynman's original wave function and Beliaev<sup>29</sup> finds that the time dependence of the quantum mechanical phase,  $\phi$ ,

is determined by the chemical potential  $\mu$ :

$$\hbar d\phi/dt = \mu \quad (22)$$

Anderson<sup>30</sup> and Donnelly<sup>31</sup> have extended this idea to studies of the critical velocity. If we have two reservoirs at different chemical potentials connected by a channel, the relative quantum mechanical phase slips at the rate

$$\hbar d(\phi_1 - \phi_2)/dt = \mu_1 - \mu_2. \quad (23)$$

Anderson points out that each time the relative phase slips by  $2\pi$  a vortex is produced. Hence vortices are produced at the rate:

$$dn/dt = (\mu_1 - \mu_2)/h. \quad (24)$$

This is the well known Josephson frequency. This says that the channel or He II film is analogous to a Josephson junction, producing vortices at the above rate.

#### B. Theories of the He Film Thickness

The transfer rate per unit circumference,  $\sigma$ , measured in beaker filling experiments, is proportional to the product of the film thickness,  $d$ , and superfluid velocity,  $v_s$ :

$$\sigma = (\rho_s/\rho) v_s d. \quad (25)$$

If the film thickness is known, properties of the critical velocity can be determined from measurements of the transfer rate. The thickness of the He film, covering a solid surface in contact with a reservoir of bulk helium, changes with the height of the film above the reservoir. By changing the height,  $h$ , of the beaker rim above the reservoir, we change the thickness of the film at the beaker rim. This is the region where dissipation takes place. In this way the dependence of the critical velocity on film thickness can be determined from measurements of the dependence of  $\sigma$  on  $h$ .

The thickness of the helium film is determined by the van der Waals attraction between the solid surface and the helium film. Schiff<sup>32</sup> has calculated the thicknesses of the film for some substrates and finds that the thickness,  $d$ , of the film at a height,  $h$ , above the reservoir is given by:

$$d = k/h^{1/3} \quad (26)$$

Here  $k$  is a constant for a given substrate material. Schiff's calculated values of  $k$  are given in Table 1.

TABLE 1  
Helium film thickness calculated by Schiff.<sup>a</sup>

$k(10^{-6} \text{ cm}^{4/3})$	Cu	Ag	Glass	Rocksalt
	4.2	4.7	$\approx 4$	2.2

<sup>a</sup>Ref. 32.

In this section the dependence of thickness on height is calculated for pure rare-gas solid substrates. Also for neon coated beakers, the dependence of the He film thickness on neon coverage is calculated.

The He film thickness is determined by a balance between van der Waals attraction to the substrate and gravitational potential energies.<sup>7,33</sup> The Mie-Lennard-Jones potential<sup>34,35</sup>,  $\phi(r)$ , is used for van der Waals potential energy between an atom in the film and an atom in the substrate:

$$\phi(r) = \epsilon(r^*/r)^{12} - 2\epsilon(r^*/r)^6. \quad (27)$$

Here  $r$  is the separation between the atoms and  $\epsilon$  is the depth of the potential well which is at an interatomic separation  $r^*$ .

We will consider atoms at the surface of the film where the separation,  $r$ , is large enough that we need only consider the

attractive part of the interaction: i.e.,  $\phi_{\text{attr}} = -2\epsilon(r^*/r)^6$ .

A helium atom a distance  $y$  from the surface of the substrate has the attractive potential energy

$$U_{\text{attr}} = n \int \phi_{\text{attr}} dV, \quad (28)$$

where  $n$  is the number density of substrate atoms and the integral is taken over the substrate. The cylindrical co-ordinate  $r'$ ,  $z'$ , and  $\theta'$  are used in a semi-infinite substrate where  $z'$  is the distance from the surface of the substrate to a plane containing  $r'$  and  $\theta'$ . Substituting for  $\phi_{\text{attr}}$  and using  $r = [r'^2 + (z' + y)^2]^{1/2}$ , we get:

$$U_{\text{attr}} = 2\epsilon n r^{*6} \int_0^{2\pi} d\theta' \int_0^\infty dr' \int_0^\infty dz' [r'^2 + (z' + y)^2]^{-3} \quad (29)$$

or,

$$U_{\text{attr}} = -\epsilon r^{*6} \pi / 3y^3. \quad (30)$$

A helium atom at the surface of a film of thickness  $d$  at a height  $h$  above the reservoir, has the additional potential energy:

$$U = mgh - \epsilon r^{*6} \pi / 3d^3. \quad (31)$$

In order for the film to be in equilibrium, the energy of a He atom must not change when it is virtually displaced from the surface of the reservoir to the surface of the film. Therefore Equation 31 can be set equal to zero and we can solve for the equilibrium film thickness as a function of height:

$$d = k/h^{1/3}, \quad (32)$$

where

$$k = (\epsilon r^{*6} \pi / 3mg)^{1/3}. \quad (33)$$

The thickness of the helium film on a rare-gas solid substrate can now be calculated. Potential parameters  $\epsilon$  and  $r^*$  are determined

from the pure rare-gas solid parameters using the coupling rules:<sup>36</sup>

$$r_{\text{He-Ne}}^* = (r_{\text{Ne-Ne}}^* + r_{\text{He-He}}^*)/2 \quad (34)$$

and

$$\epsilon_{\text{He-Ne}} = (\epsilon_{\text{Ne-Ne}} \epsilon_{\text{He-He}})^{1/2}. \quad (35)$$

Values for the pure rare-gas parameters are given in Table 2 with the number density,  $n$ , evaluated at absolute zero. Values of the parameters for the interaction of helium with rare gas atoms are given in Table 3. The parameters in Table 3 are calculated using Equations 34 and 35 and Table 2.

TABLE 2  
Values of the Mie-Lennard-Jones potential parameters  $\epsilon$  and  $r^*$  and number density  $n$  for rare-gas solids and liquid helium.

	$\epsilon/k(K)$	$r^* (\text{\AA})$	$n(10^{22}/\text{cm}^3)$
He <sup>a</sup>	10.2	2.89	2.18
Ne <sup>b</sup>	36.3	3.16	4.54
Ar <sup>b</sup>	119	3.87	2.66
Kr <sup>b</sup>	159	4.04	2.22
Xe <sup>b</sup>	228	4.46	1.73

<sup>a</sup>Ref. 5.

<sup>b</sup>Ref. 34.

TABLE 3  
Values of the Mie-Lennard-Jones potential parameters  $\epsilon$  and  $r^*$  for the interaction of helium with rare gas atoms.

	He-Ne	He-Ar	He-Kr	He-Xe
$\epsilon/k(K)$	19.2	34.9	40.3	48.3
$r^* (\text{\AA})$	3.02	3.38	3.46	3.68

One additional correction is made before values are calculated for the thickness. Correction is made for the helium displaced by



the substrate since we are interested in the additional attraction of the substrate as compared to pure helium:

$$U_{\text{attr}} = U_{\text{He-Ne}} - U_{\text{He-He}} \quad (36)$$

Values of  $k$ , obtained when this corrected  $U_{\text{attr}}$  is substituted in Equation 31, are given in Table 4.

TABLE 4  
Calculated thickness of He film on rare-gas solid substrate.

$k(10^{-6} \text{ cm}^{4/3})$	Ne	Ar	Kr	Xe
	2.3	3.0	3.1	3.5

In the experiments, neon coated glass beakers are used rather than pure neon beakers. The neon coverage necessary to have an effective neon beaker is now calculated. Because the interaction between helium and glass is not known, the calculation is done for a neon coated xenon beaker. It is assumed that these calculated results are qualitatively valid for glass as well as xenon.

To calculate the He film thickness for a neon coated xenon beaker, the attractive potential is integrated over the Ne layer and over the semi-infinite Xe substrate. Correcting again for the displaced helium, the attractive potential energy is

$$U_{\text{attr}} = U_{\text{He-Xe}} + U_{\text{He-Ne}} - U_{\text{He-He}} \quad (37)$$

For a neon layer having thickness  $\xi$ , the potential energy terms, in Equation 37, are for a He atom a distance  $y$  from the surface:

$$U_{\text{He-Xe}} = \epsilon_{\text{He-Xe}} \frac{r_{\text{He-Xe}}^*}{r_{\text{He-Xe}}} \frac{\pi n_{\text{Xe}}}{3(y + \xi)^3}, \quad (38)$$

$$U_{\text{Ne-Ne}} = \epsilon_{\text{He-Ne}} \frac{r_{\text{He-Ne}}^*}{r_{\text{He-Ne}}} \frac{\pi n_{\text{Ne}}}{3} [1/3y^3 - 1/3(y + \xi)^3], \quad (39)$$

and

$$U_{\text{He-He}} = \epsilon_{\text{He-He}} \frac{r_{\text{He-He}}^*}{r_{\text{He-He}}} \frac{\pi n_{\text{He}}}{3y^3}. \quad (40)$$

The potential energy,  $U_{\text{attr}}$ , is, as before, equated to the gravitational potential energy giving the thickness of the He film. However, when this  $U_{\text{attr}}$  is substituted in Equation 31, it can not be easily solved for  $d$  as a function of height. Since this is a small correction, we solve for the thickness at  $h = 1$  cm. This thickness is taken to be numerically equal to  $k$  and the functional form of Equation 26 is assumed.

The resulting thickness with  $h = 1$  cm, as a function of neon coverage,  $\xi$ , is shown in Figure 1. For  $\xi < 10 \text{ \AA}$ , the thickness of the He film is equal to the thickness over a pure Xe substrate. For  $\xi > 1000 \text{ \AA}$ , the thickness of the He film is equal to the thickness over a pure Ne substrate so that we have an effective Ne beaker. One-half saturation, where the He film has the average of these thicknesses, occurs at  $\xi = 100 \text{ \AA}$ .

The thickness as a function of Ne coverage, as shown in Figure 1, is assumed to be qualitatively valid for a glass substrate instead of Xe substrate. That is, we assume that we need only put a  $1000 \text{ \AA}$  neon layer on a glass beaker to have an effective Ne beaker.

Dzyaloshinskii *et al.*<sup>37</sup> have objected to the use of the Mie-Lennard-Jones potential for a solid interacting with a liquid. They point out that the Mie-Lennard-Jones potential is strictly valid only for isolated atoms and that corrections must be made for the screening of neighboring atoms. This requires knowing the entire electromagnetic spectrum of both the helium and neon. This is beyond the scope of this thesis. However, the correction should be smallest for the case of neon substrate.

The simple calculation above is for a static film interacting

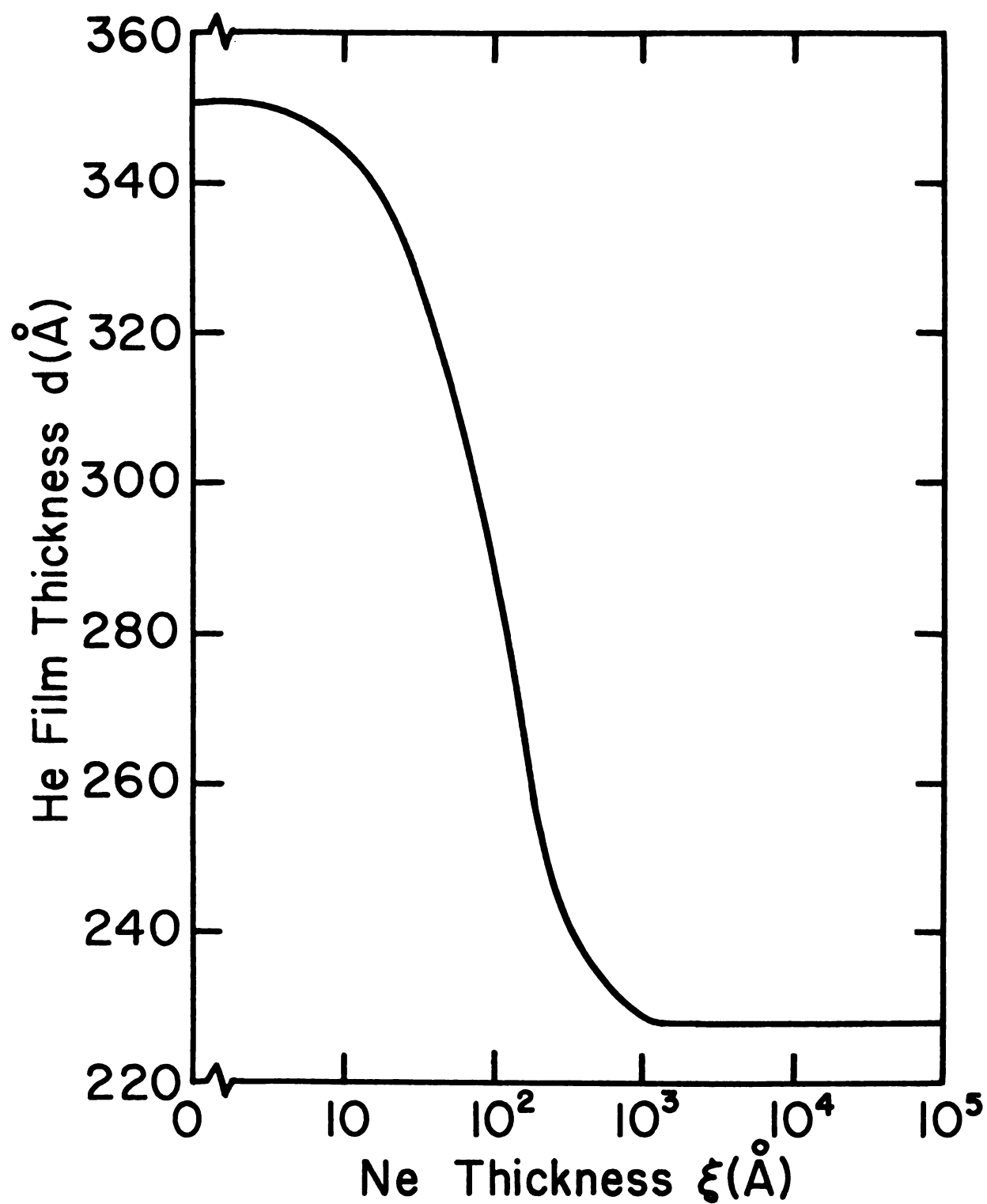


Figure 1: Calculated thickness of the helium film,  $d$  with  $h = 1$  cm, versus thickness of Ne coating,  $\xi$ , on a Xe substrate.

with an infinite wall. Kontorovich<sup>38</sup> predicted that the thickness of a moving film would be less than the thickness of a static film. However, Keller<sup>39</sup> has found experimentally that the thicknesses are the same. Goodstein and Saffman<sup>40</sup> have considered the theory of a moving film in more detail and find that both moving and static films have the same thickness as is determined by Equation 31 above.

Various methods have been used to measure the thickness of the film experimentally.<sup>4</sup> Bowers<sup>41</sup> has weighed the film adsorbed on a metal foil. Atkins<sup>42</sup> has calculated the thickness of the film from measurements of oscillations of the film. Keller<sup>39</sup> has also measured the thickness, using a capacitance technique which is sensitive to changes in the thickness.

The most direct and accurate measurements of the helium film thickness are by L. C. Jackson and co-workers.<sup>4</sup> They measure the ellipticity of light reflected from a surface that is covered by the He film. Ham and Jackson<sup>43</sup> find that the thickness parameter,  $k$ , is equal to  $3.0 \times 10^{-6} \text{ cm}^{4/3}$ . This is the basic measurement that is used for the thickness of the He film on a glass substrate in this thesis.

### C. Dynamics of the Film Transfer

Dynamical limitations to measurements of the properties of critical velocity in beaker filling experiments are examined in this section. The flow is considered to take place in a channel having the vertical cross-section  $d = k/h^{1/3}$ , as discussed before. In the experiment, the rate at which the beaker fills is measured. The transfer rate per unit circumference,  $\sigma$ , is related to the velocity of the inner level,  $dz/dt$ , for a beaker of radius  $r$ , by:

$$\sigma = (r/2)dz/dt. \quad (41)$$

These measurements of  $\sigma$  are related to the superfluid velocity by

$$\sigma = (\rho_s/\rho)v_s d. \quad (42)$$

The superfluid obeys the two fluid equation, Equation 2:

$$d\vec{v}_s/dt = -(1/\rho)\vec{\nabla}P + s\vec{\nabla}T. \quad (43)$$

In the case of isothermal, irrotational flow, as we have for film transfer at subcritical velocities, this becomes:<sup>42</sup>

$$d\vec{v}_s/dt = \partial\vec{v}_s/\partial t + (\vec{v}_s \cdot \vec{\nabla})\vec{v}_s = -(1/\rho)\vec{\nabla}P. \quad (44)$$

For a co-ordinate  $l$  parallel to the surface of the beaker and parallel to  $\vec{v}_s$ , this becomes:

$$\frac{\partial}{\partial t} v_s + \frac{\partial}{\partial l} \left( \frac{1}{2} v_s^2 \right) = -\frac{1}{\rho} \frac{\partial P}{\partial l} \quad (45)$$

Integrating along the path  $l$  from the outside level of the beaker to the inside level, we get:

$$\int (\partial v_s / \partial t) dl + \left( \frac{1}{2} v_s^2 \right) \Big|_{\text{outside}}^{\text{inside}} = -(1/\rho)\Delta P = -gz, \quad (46)$$

where  $z$  is the level difference. Because of the nearly zero velocity inside and outside of the beaker, the second term on the left hand side of Equation 46 drops out. Using the continuity equation,

$$v_s d = \text{constant along path}, \quad (47)$$

and substituting for  $v_s$  in terms of  $dz/dt$  from Equation 41, we get

$$M^* d^2 z / dt^2 = -\rho g z, \quad (48)$$

where  $M^* = (\rho^2/2\rho_s) \int (r/d) dl$ . This relates the acceleration of the measured level difference to the driving pressure,  $\rho g z$ , for sub-critical flow.

To account for the critical velocity, we add a frictional

pressure,  $P_g$ , to the right hand side of Equation 48:<sup>20</sup>

$$M^* d^2z/dt^2 = P_g - \rho gz. \quad (49)$$

We are primarily interested in the frictional pressure as a function of superfluid velocity,  $v_g$ , or transfer rate,  $\sigma$ . This can be measured directly for low acceleration and large  $z$ . In this case  $M^* d^2z/dt^2$  is small compared to  $\rho gz$  so that Equation 49 says that the frictional pressure is equal to the observed driving pressure, *i.e.*,  $P_g = \rho gz$ .

For small  $z$  and large acceleration, the acceleration term becomes important so that the frictional pressure cannot be measured directly. In this case  $P_g$  is small and the levels oscillate with small damping.<sup>14,42</sup> The apparatus used in this thesis, however, is not suitable for studying these oscillations.

### III. EXPERIMENTAL

#### A. Clean Glass Substrate Apparatus.

Atkins<sup>44</sup> in 1948, and van den Berg and de Haas<sup>45</sup> independently in 1949, reported transfer rates as much as twenty times larger than those originally reported by Daunt and Mendelssohn.<sup>13</sup> Bowers and Mendelssohn<sup>46</sup> showed that these enhanced transfer rates were a result of impurities, such as air, condensed on the beaker surface.

These enhanced transfer rates for contaminated beakers can arise either from an increased film thickness or an increased microperimeter of the beaker. In the case of a granular impurity, the microperimeter is larger than the apparent macroperimeter and, in addition, a thicker film can result from liquid helium held between the grains by surface tension. McCrumb and Eisenstein<sup>47</sup> pointed out that polar impurities, such as water, can also result in a thicker film. The thick film, in this case, is a result of a stronger attractive force, of the polar substrate to the helium, than the usual van der Waals forces.

Smith and Boorse<sup>17</sup> investigated these problems in more detail. They found that, by being careful to prevent impurities, the enhanced transfer rates could be eliminated but a, typically 10%, background variation in the transfer rate remained. These variations prevented them from seeing a dependence of the transfer rate on substrate

material for the materials they investigated.

The apparatus used in this thesis was designed to provide a very clean, and vibration free, environment for the beaker in order to minimize these problems. To do this the beaker was enclosed in an experimental chamber rather than exposing it to the possibly dirty environment of the liquid helium bath. In addition, rather than condensing possibly impure helium gas into the experimental chamber, the chamber was filled by admitting helium in liquid form from the bath. Another advantage of the chamber was that the helium level of the chamber remained constant, while the beaker was filling, whereas the helium level of the bath decreased slowly with time.

The experimental chamber and beaker are shown in Figure 2. A 2 in. Kovar to glass seal was used to make the chamber. The chamber was demountable at the top by means of brass flanges that were sealed with a lead O-ring. Five ampere fuse wire was used to make the O-ring whose ends were soldered together to form a closed loop. Liquid helium was admitted to the chamber through the needle valve at the top of the apparatus. This valve was made from a Hoke #3242 M 4B needle valve which was modified to reduce its mass.

Connections from outside the dewar to the experimental chamber were made with a 3/8 in. o.d. stainless steel tube. Two other 3/8 in. stainless steel tubes served as supports for the chamber. Connections were made from the experimental chamber to mercury and oil manometers, a mercury bubbler, and a diffusion pump system. The manometers were used to measure the vapor pressure of the liquid helium in the chamber in order to determine its temperature. The bubbler served as a vacuum tight, safety valve which would allow



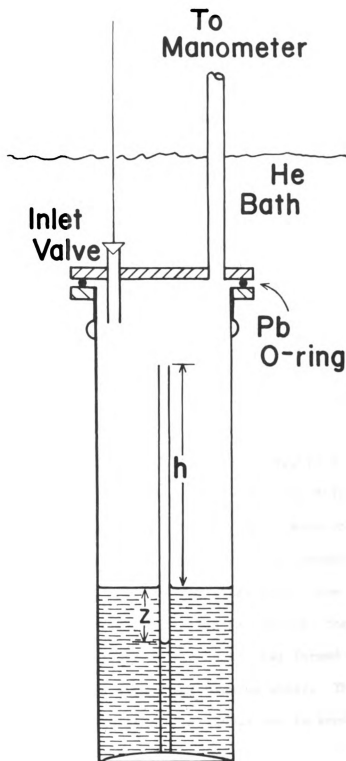


Figure 2: Schematic drawing of clean glass substrate apparatus.

helium gas to escape from the chamber in case of pump failure.

The diffusion pump system consisted of a CVC model 21, air cooled diffusion pump which was backed by a Welch model 1402 B, 140 liter per minute mechanical pump. An, approximately 2 liter capacity, liquid nitrogen cold trap placed between the pumps and apparatus, served as a cryopump and in addition prevented pump oil from diffusing to the beaker. Before each run the diffusion pump system was used to degas the beaker. After each run the mechanical pump, without the diffusion pump, was used to remove the liquid helium from the experimental chamber.

Pressures above  $10^{-3}$  Torr, in the diffusion pump system, were measured with a CVC model GP-140 pirani gauge. Pressures below  $10^{-3}$  Torr were measured with an H. S. Martin cold cathode ionization gauge. The highest vacuum attainable with this system was about  $10^{-6}$  Torr.

Beakers used in these experiments, shown in Figure 2, were made of 3 mm i.d., 5mm o.d., and 10 cm height Corning #7740 Pyrex tube. The beaker was mounted on a 1 1/2 in. Pyrex base which had small Pyrex hooks for removing the beaker from the demounted chamber. Care was taken to specially select glass tube, from the stock of glass at the M. S. U. Glass Fabrication Laboratory, that was clean and scratch free. The rim of the beaker was formed by carefully cutting the Pyrex tube with a Carborundum wheel. The rim was then lightly fire-polished to remove scratches and to smooth the edges.

The exact radius of the beaker was determined volumetrically. The mass of room temperature, distilled water in the beaker was

measured as a function of height with a Mettler analytical balance. Using the density of water, the resulting volume versus height curve was plotted and was fit by a least squares straight line. The slope of this curve gave the cross-sectional area of the inside of the beaker from which the inner radius was determined. Two different, but otherwise identical, beakers were used in these experiments. Beaker 1 has an inside radius of 0.162 cm and beaker 2 had an inside radius of 0.156 cm.

When the Pyrex beaker was removed from the demounted chamber, it could be cleaned in solvents that were not compatible with the metal parts of the apparatus. The following cleaning procedure gave reproducible transfer rates and was used before each run during the clean glass substrate study:

The beaker was first rinsed with distilled water and then with methanol. This was followed by cleaning with detergent in an ultrasonic bath and rinsing ultrasonically with distilled water. The beaker was then rinsed with nitric acid and rerinsed with distilled water. It was then heated to 200 °C in air with a heat gun to remove adsorbed water. Finally, it was mounted in the experimental chamber and heated to roughly 75 °C with an infrared heat lamp while pumping to about  $10^{-6}$  Torr with the diffusion pump system. The pumping was continued for one or two days prior to cooldown.

The entire cleaning procedure above may not be necessary before each run. Allen and Armitage<sup>48</sup> have used a similar cleaning procedure and report that, after the initial thorough cleaning, only heating and pumping between runs is necessary. With the neon substrate apparatus, described in the next section, it was also found

that it was only necessary to prevent impurities from entering the chamber and to diffusion pump between runs after the initial thorough cleaning.

Impurity problems were encountered in the preliminary runs before the actual thesis data were taken. It appeared that the beaker in the original non-demountable apparatus got dirtier each time it was cleaned, *i.e.*, the transfer rate increased after each cleaning. This was most likely a result of water, used in the cleaning procedure, being adsorbed on the beaker. These problems led to the design of the demountable apparatus so that the beaker could be removed to be cleaned in stronger solvents and to be heated to higher temperatures. These observations with the non-demountable, demountable, and neon substrate apparatuses indicate that the crucial step in the cleaning procedure is heating to 200 °C to remove adsorbed water.

Although these observations indicate that the beaker may have to be cleaned thoroughly only once, the cleaning procedure, nevertheless, was used with slight variations before each run as a test of the reproducibility of the cleaning procedure. This also ensured that the maximum initial cleanliness was reached.

The experimental chamber was immersed in a liquid helium bath in an H. S. Martin, glass, liquid helium dewar with a removable liquid nitrogen dewar. Both the nitrogen and helium dewars were strip silvered with 3/4 in. viewing slits. Liquid helium bath temperatures were lowered by evacuating the helium dewar with a Heraeus-Engelhard #E225, air-cooled, 147 cfm vacuum pump. The temperature of the helium bath was regulated to better than  $\pm 0.01$  K

for temperatures above 1.5 K with a Cryonetics Mark II mechanical pressure regulator. Comparable temperature regulation was achieved for temperatures near 1.3 K by regulating the pumping speed with a 2 in. gate valve in the pumping line. The lowest temperature attainable with this apparatus was about 1.2 K.

Vibrations of the apparatus were minimized by placing flexible bellows along the pumping line. A 4 in. x 24 in. copper bellows was located in the main 4 in. pumping line near the pump which was about 15 ft. from the apparatus. Also an asymmetric arrangement of five automobile radiator hoses connecting the helium dewar to the 4 in. pumping line further reduced vibration. Three 2 in. x 15 in. hoses, one 1 1/2 in. x 12 in., and one 1 1/2 in. x 5 in. hose were used in this arrangement.

Two different means of illuminating the beakers during these experiments gave identical results. This agrees with the results of Bowers and Mendelssohn<sup>46</sup> and Picus,<sup>49</sup> who found that the transfer rate was independent of the intensity of the illuminating radiation, as long as it was not too intense. For this experiment, radiation, other than that used for illumination, into the dewar was minimized by placing radiation shields, made of aluminum foil, in the helium bath. These shields were placed above the apparatus and around it, except for vertical viewing slits. Additional shielding was provided by covering the slits on the outside of the nitrogen dewar with aluminum foil except for 6 in. near the bottom which was left uncovered for viewing.

The first means of illumination made use of an 8 watt fluorescent light. This light was shielded by a plastic diffuser which, except for a narrow slit, was covered with aluminum foil. In

addition, a green glass filter was placed in front of this slit. Infrared radiation from this light source was filtered by a water cell placed in front the dewar slit. Using this illumination the experiment was done with the laboratory completely dark except for other low intensity lights which illuminated the laboratory notebook and instruments.

A second, more convenient method of illumination used no special light source. In this case illumination was provided by room light with the laboratory slightly darkened. Radiation shields on the nitrogen dewar and in the helium bath were again used in this arrangement.

#### B. Neon Substrate Apparatus

Neon beakers were made by coating clean glass beakers with neon. To have an effective neon beaker, as was discussed in section II-B, a  $1000 \text{ \AA}$  or greater thickness neon coating on the glass beaker is required to saturate the forces between the helium and substrate material. However, the coating must be smooth and uniform to avoid the rough substrate problems that were discussed in the previous section.

The neon substrate apparatus is similar to the clean glass substrate apparatus except that, in order to raise the temperature of the chamber above 4 K, it was provided with a vacuum space and heating coil. If neon is condensed directly onto a surface having a temperature of 4 K, enhanced transfer rates are seen presumably due to rough substrate conditions. This was observed in preliminary experiments. The rough substrate in this case was most likely a result of the fact that neon atoms stick, as soon as they strike,

a 4 K surface.<sup>50</sup> At higher surface temperatures, near 20 K for neon, the adsorbed neon atoms are distributed more uniformly because they have a lower probability of sticking when they strike the surface. Also because of their thermal energy, the adsorbed neon layers, at these temperatures, are somewhat mobile and as a result are able to smooth themselves.<sup>51</sup> Therefore the apparatus was designed so that the neon could be condensed with the temperature of the glass beaker in the range 20K to 25 K.

The neon substrate apparatus is shown in Figure 3. The inner chamber, containing the beaker, was made from a 1 1/2 in. Kovar to glass seal. The outer chamber, used to form a vacuum space around the inner chamber, was made from another Kovar to glass seal of 2 in. diameter. The tops of both chambers were soldered to brass flanges.

Two 1/2 in. stainless steel tubes supported the apparatus. One of these tubes served both as an inlet to the vacuum, or exchange gas, space and as an outlet for electrical leads from the heater and thermometer. The other 1/2 in. tube formed a vacuum space around a 1/4 in. stainless steel tube which served as an outlet from the inner chamber. The tube from the inner chamber, as in the clean glass substrate apparatus, was connected to mercury and oil manometers, the mercury bubbler, and the diffusion pump system.

Liquid helium was admitted to the inner chamber from the bath through a 1/8 in. copper tube from the needle valve at the top of the outer chamber. The needle valve used in this apparatus was constructed by the M. S. U. Physics Department Machine Shop.

These chambers were not easily demountable so that the beaker,

A	Outer tube from inner chamber
B	Exchange gas and wires
C	Needle valve
D	Pt thermometer
E	Vacuum space
F	Outer chamber
G	Inner chamber
H	Beaker
I	Heater



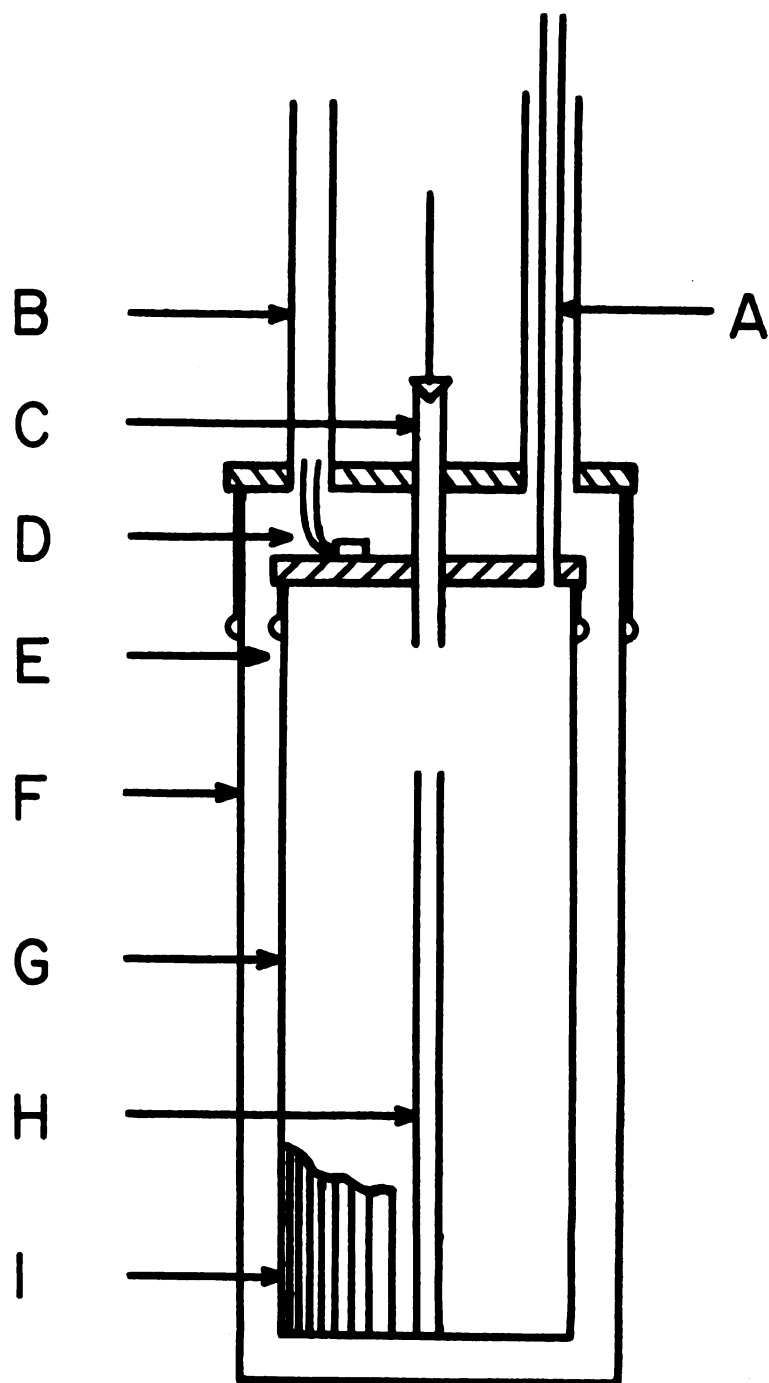


Figure 3: Schematic drawing of Ne substrate apparatus.

which was fastened to the inner chamber, could not be removed for cleaning before each run. The beaker was initially cleaned and heated using the procedure given in the previous section. The inner chamber was then assembled taking care not to get the beaker dirty. Transfer rates obtained with the assembled apparatus were the same as those obtained during the clean glass study. This indicated that the beaker was not contaminated during the assembly of the inner chamber.

As was discussed in the previous section, the beaker was kept clean between runs by pumping. Occasional runs were made without a neon coating during the course of the neon substrate study. The transfer rates observed in these runs were again the same as the transfer rates obtained during the clean glass study. This demonstrated that the glass beaker in the neon substrate apparatus remained clean during the neon substrate study.

The exact inner radius of the beaker was again determined volumetrically. Because the beaker was fastened to the massive inner chamber it could not be calibrated directly. Another beaker, made from the same section of glass tube that was used in the construction of the experimental beaker, was used for calibration. The inner radius of this beaker was found to be 0.160 cm.

Manganin resistance wire having a resistance of 10 ohms per foot was used for the heating coil. Approximately 100 feet of this wire was wound longitudinally around the inner chamber, and the base of inlet tubes, leaving vertical slits for viewing the beaker. Nylon thread and masking tape were used to fasten the heater wire to the inner chamber. The ends of the heater wire were connected

to a small terminal strip at the top of the inner chamber in the vacuum space. The leads from the terminal strip were routed through the exchange gas tube and were connected to 2 pins of a vacuum tight, 9 pin connector at room temperature.

A miniature platinum resistance thermometer was used to measure the temperature of the inner chamber. The thermometer used in this apparatus was an Artronix #PS-1 which had the serial number X-159. The thermometer had a square cross-section, 0.2 in. on a side, and was 0.05 in. thick. Thermal contact between the brass top of the inner chamber and the thermometer was made using Apiezon N vacuum grease. The bottom of the terminal strip, used for connecting electrical leads, held the thermometer in place.

The resistance of the platinum resistor as a function of temperature was calibrated from basic measurements of the resistance at 4.2 K and 273 K. These two measurements of the resistance were made with the apparatus immersed in a liquid helium bath, at atmospheric pressure and, an ice and water bath, respectively. The resistance,  $R$ , as a function of temperature,  $T$ , is then given by

$$R(T) = R_{4.2 \text{ K}} + Z(T)(R_{273 \text{ K}} - R_{4.2 \text{ K}}). \quad (50)$$

Here  $Z(T)$  is a tabulated function given by White<sup>52</sup> for Pt.

The miniature Pt resistance thermometer had only two short leads. In order to eliminate lead resistance, it was converted to a four-lead arrangement by connecting it to four inlet leads at the terminal strip. Two of these leads supplied a 1 mA current to the resistor and the other two leads served as zero current, potential leads. These four leads also were routed up the exchange gas tube and were connected to four other pins of the nine pin connector.

The resistance of the thermometer was measured by connecting the potential leads from the nine pin connector to a Leeds and Northrup model K-3 potentiometer. The auxiliary emf terminals of this potentiometer were used to monitor the 1 mA current through the platinum resistance thermometer. This was done by measuring the potential difference across a one ohm standard resistor which was in series with the resistance thermometer.

The heater leads from the nine pin connector were connected to a Variac variable ac voltage source. A 1000 ohm resistor was placed in series with the heater and Variac to reduce the heat input. Temperature regulation, for temperatures above 4 K, was achieved by manually regulating the voltage output of the Variac. This was done by adjusting the voltage while variations of the resistance of the thermometer, from the value set on the potentiometer, were monitored on the dc potentiometer null detector.

While the neon was being condensed, the chamber temperature was above 4 K and a vacuum was maintained in the vacuum, or exchange gas, space. After the neon had been condensed, the inner chamber was brought to a temperature of 4 K. At this time helium gas was admitted to the vacuum space before admitting liquid helium to the inner chamber.

The helium exchange gas was stored at atmospheric pressure in a one-half liter, glass flask outside the dewar. A glass, vacuum stopcock was opened to admit the exchange gas to the evacuated vacuum space. This procedure ensured that the exchange gas pressure would never exceed atmospheric pressure even when the apparatus was warmed to room temperature. In addition, the stopcock served as a safety

valve in case liquid helium should leak into the vacuum space from the bath.

The amount of neon needed to coat the beaker was determined by assuming that the neon uniformly covered all the surfaces of the beaker and the inside surfaces of the inner chamber. Using the area of these surfaces, the amount of, room temperature, neon gas required to form a desired thickness was easily calculated.

The neon gas required to form a desired thickness neon coating was stored in a one liter glass flask outside the dewar. Typically a 1000 Å coating was used which required a room temperature, neon pressure of 5.3 Torr in the storage flask. The gas handling system for the neon is shown schematically in Figure 4. Mercury and oil manometers were used to measure the pressure of the neon. After the desired partial pressure of neon was admitted to the flask, helium gas was added filling the flask to a pressure of one atmosphere.

Matheson Research grade neon having a purity of 99.999% was used in these experiments. The helium gas having an estimated purity of at least 99.99% was obtained from the M. S. U. Physics Department. The purity of the helium gas was tested by admitting only helium gas, without neon, to the experimental chamber. It was then observed that the transfer rate was the same as for clean glass. This demonstrated that no impurities from the helium gas that was mixed with the neon gas were condensed on the beaker surface.

During a run, the helium and neon gas mixture was admitted to the experimental chamber with the initial chamber temperature at 25 K. The helium gas served both to distribute the neon and to

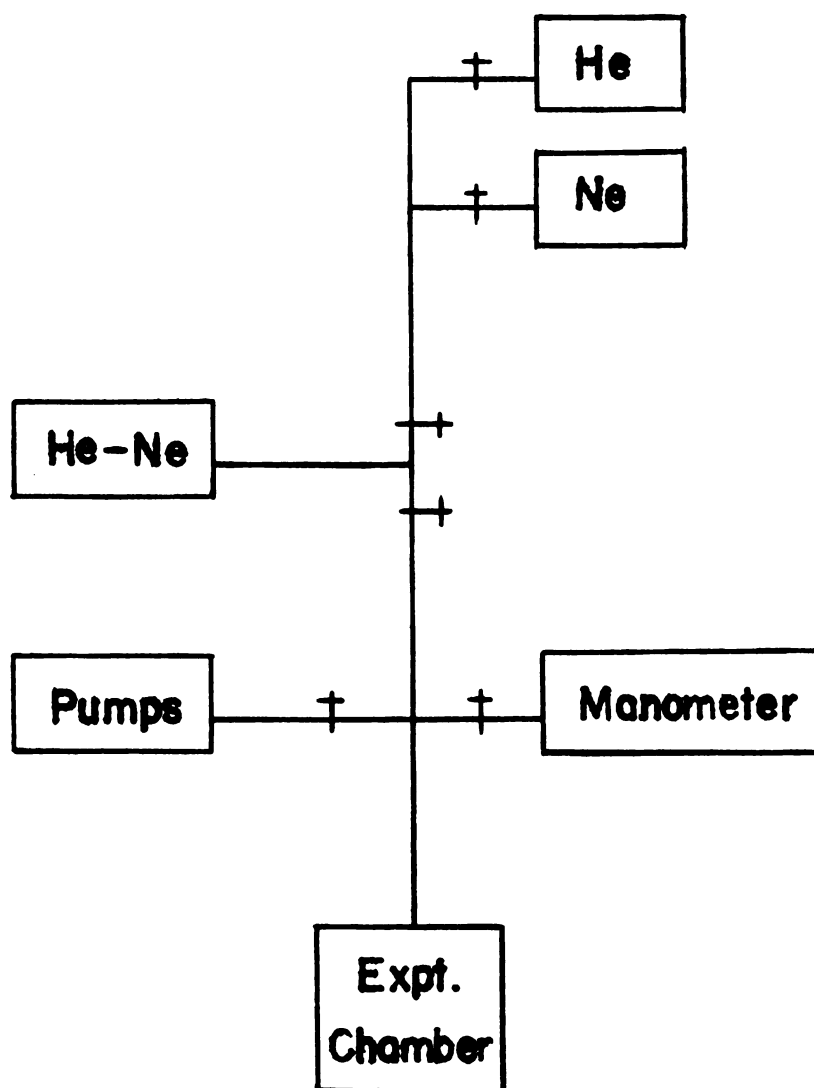


Figure 4: Gas handling system for Ne.

maintain thermal equilibrium within the chamber. After the gases were admitted to the chamber, the chamber temperature was then lowered at a rate of 0.2 K/min from 25 K to 4 K condensing the neon on the beaker. Transfer rate data indicate that this procedure resulted in a smooth surface for coverages of about  $1000 \text{ \AA}$ , although no independent test of the surface was made.

For the condensation of the neon, the liquid helium level in the dewar was set about half way up the outside of the experimental chamber. The tube from the inner chamber to the needle valve provided thermal contact between the inner chamber and the helium bath. The heat from the inner chamber was dissipated primarily in the cold helium vapor surrounding the top of the outer chamber. Heat was also dissipated in the liquid helium by heat conduction down the glass walls of the outer chamber.

The liquid helium transfer tube from the storage dewar to the experimental dewar remained connected during the neon condensation. A slight overpressure on the storage dewar maintained a slight flow of cold helium gas through the transfer tube to the experimental dewar. This cold gas served two purposes. It, first of all, maintained a stream of cold gas on the top of the apparatus to provide cooling to the inner chamber. In addition, this cold gas kept the transfer tube cold so that more liquid helium could be transferred after the condensation of the neon without warming the apparatus.

### C. Experimental Procedure

The measurements made during an experimental run to determine the He film transfer rate are described in this section. As was described in the previous two sections, the surface of the beaker

was prepared for running before liquid helium was admitted to the experimental chamber. This preparation involved, in the clean glass substrate study, thoroughly cleaning the glass beaker one or two days prior to cooldown. In addition, during the neon substrate study, a layer of neon was carefully condensed on the surface of the beaker before admitting liquid helium to the experimental chamber.

During an experimental run, approximately four liters of liquid helium were transferred into the experimental dewar and cooled by pumping to the desired temperature. Liquid helium was then admitted to the experimental chamber from the bath, by means of the needle valve, filling the chamber outside the beaker to a depth of about 2 cm.

The position of helium level inside the beaker was then measured as a function of time until the inner and outer beaker levels reached equilibrium. Usually the level difference,  $z$ , was monitored over a distance of 1 1/2 cm which took a period of time of about 30 minutes. While the beaker was filling, the outer level remained at a nearly constant distance  $h$  below the beaker rim. The position of the inner and outer levels with respect to the beaker along with the distances  $h$  and  $z$  are shown in Figure 2.

The positions of the helium levels were measured with an elegant Wild-Heerbrug model KM326 cathetometer. During a beaker filling, the position of the inner beaker level was measured and recorded as a function of time with an accuracy of 0.001 cm taking height versus time readings usually every 30 sec. The time during the beaker filling was measured with a stopwatch. The stopwatch was started at the time of the first height reading and subsequent



readings were made with an accuracy of  $\pm 1$  sec without stopping the stopwatch.

Figure 5 shows the level difference,  $z$ , as a function of time for three of five beaker fillings at different  $h$ 's during the same run. The transfer rate is proportional to the derivative of the  $z(t)$  curve. We notice that these curves are nearly straight and have only slightly different slopes. This agrees with the original observations of Daunt and Mendelsohn<sup>13</sup> that  $\sigma$  is nearly independent of pressure head,  $z$ , and height,  $h$ , of the beaker rim above the reservoir.

However this thesis is concerned with the slight departures of  $\sigma$  from this simple behavior. These curves in Figure 5 are slightly concave downwards reflecting the dependence of  $\sigma$  on  $z$ . Also the height dependence of  $\sigma$  is manifested in the different slopes of the curves taken at different  $h$ 's.

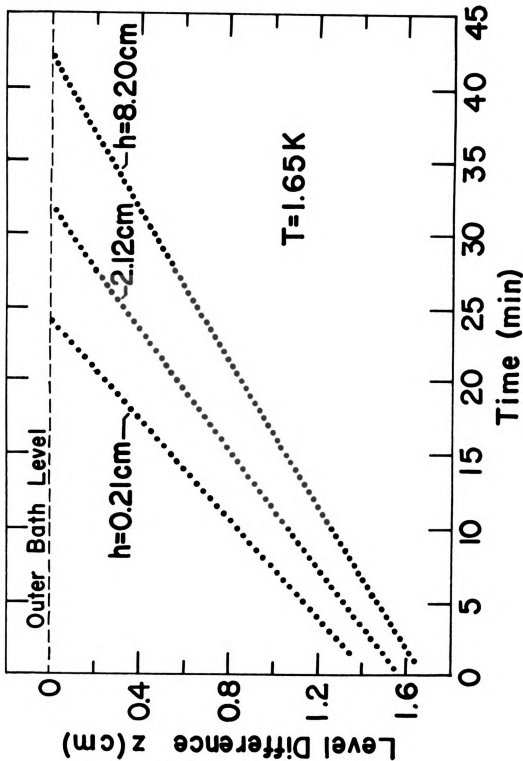


Figure 5: Level difference,  $z$ , as a function of time for three beaker fillings at three different heights,  $h$ , to the beaker rim.

#### D. Data Reduction and Experimental Accuracy

The transfer rate per unit circumference,  $\sigma$ , is proportional to the derivative of the  $z(t)$  curves shown in Figure 5 of the previous section, *i.e.*,

$$\sigma = (r/2) \, dz/dt. \quad (51)$$

Here  $r$  is the inside radius of the beaker. In this section the computer method that is used to evaluate these derivatives or transfer rates is discussed. In addition, the random error in  $\sigma$  from the measurements and the differentiation procedure is estimated.

The data reduction was done using the computer terminal in the Physics - Astronomy Building. This terminal was connected to the Michigan State University, Control Data Corporation 6500 computer which was located in the Computer Center.

The following procedure is used in the computer program to calculate the derivatives.<sup>53</sup> A quadratic equation,

$$z(t) = A + Bt + Ct^2, \quad (52)$$

is fit to the first eleven data points of a beaker filling. The derivative,

$$dz/dt = B + 2Ct, \quad (53)$$

is then evaluated at datum point number 6, the midpoint of the eleven data point segment. Next, data points 2-12 are fit in the same way and the derivative is evaluated at the midpoint of this segment. By taking overlapping segments of the  $z(t)$  curve in this manner, the derivative of the curve can be determined either as a function of  $z$  or  $t$ .

Transfer rates,  $\sigma$ , are then obtained by multiplying the derivatives by  $G = (r/2) \times 10^{-5}$ . This gives  $\sigma$  in units of  $10^{-5} \text{ cm}^3/\text{sec-cm}$

so that  $\sigma$  is numerically between 1 and 10. Figure 6 shows  $\sigma$  as a function of  $z$  for a typical run. Each point on this curve was obtained by evaluating the derivative, which was then multiplied by  $G$ , at the midpoint of one of the overlapping eleven data point segments. The solid curve is a fitted curve which shows the trend of data. This curve will be discussed in the next section.

Details of the computer program, Sigma-z, are given in Appendix A. A Fortran listing of the program Sigma-z is given in Table A1. Table A3 gives the computer output for these data. Although the data for only one beaker filling are shown in Appendix A, the program was designed so that data from several beaker fillings could be submitted and analyzed at the same time.

The first computer card of the input data in Table A2 gives an identification number for the data set. The second computer card of the input gives the height of the helium level outside the beaker,  $H_o$ , and the geometrical factor  $G$ . Subsequent cards give the position of the inner level as a function of time. Six height versus time data points are recorded on each computer card. The remaining points, which do not fill one card, are then recorded one datum point per computer card.

The first line of the computer output presented in Table A3 gives the identification number of the run; the liquid helium level outside the beaker,  $H_o$ ; and the geometrical factor,  $G$ . Two other numbers given on this line of the output are the parameters  $A$  and  $B$  which describe the  $\sigma(z)$  curve. These parameters are discussed in the next section.

The remaining computer output is presented in eight columns

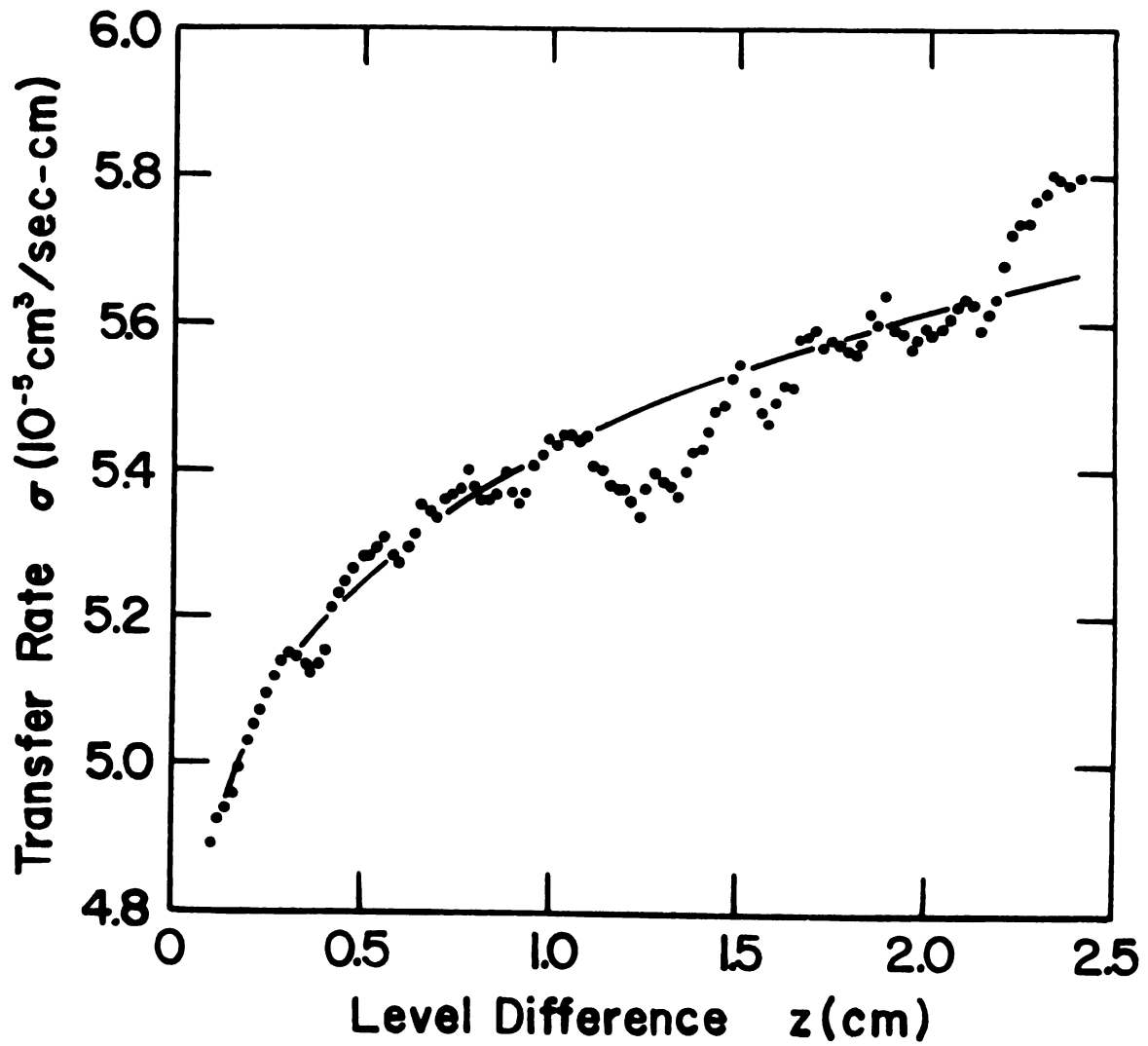


Figure 6: Transfer rates,  $\sigma(z)$ , from the  $z(t)$  curve of a typical run.

in Table A3. The second and third columns of the Table list the input data, *i.e.*, the inside beaker level height,  $H$ , versus time. These data points are numbered in column 1. The fourth column gives the nearly constant difference in the inside beaker level height between adjacent data points for proofreading purposes. The transfer rate,  $\sigma$ , as a function of  $z$  is presented in tabular form in columns 5 and 6. In the next section the functional form of the  $\sigma(z)$  curve is considered. In that section use is made of the curve  $1/\sigma$  versus  $\ln z$  which is tabulated in columns 7 and 8.

The random errors in the  $\sigma(z)$  points, arising from the measurements and the differentiation procedure, are now estimated for the  $\sigma(z)$  points of a particular beaker filling such as these shown in Figure 6. To do this, the root mean square deviation of the  $z(t)$  data points from the fitted quadratic equation was calculated for the overlapping segments of a few typical sets of beaker filling data. Since the  $z(t)$  curve is nearly a straight line, the error in the derivative of the eleven data point segment was taken to be the difference in the slopes of two straight lines whose end points differed in  $z$  by twice the rms deviation. Using the difference in time of 300 sec between the first and eleventh data points, the error in the derivative is estimated to be  $\pm 2\Delta/300$  sec, where  $\Delta$  is the rms deviation. The average percent error for the overlapping segments of these  $z(t)$  curves was found to be about 0.6%. This agrees with the error that would be estimated for the derivative using the accuracy  $\pm 0.001$  cm for the cathetometer readings.

The percent error of  $\sigma$  is the sum of the percent errors of the derivative and the beaker radius. From the volume versus height

curve used in calibrating the beaker, random deviations in the radius of the beaker along its length are estimated to be  $\pm 0.2\%$ . This error has, however, already been taken into account in the derivative error because the derivative error was estimated from experimental data. Therefore the random error in the  $\sigma(z)$  points for one beaker filling is estimated to be  $0.6\%$ .

There are also larger run-to-run differences in the transfer rate which arise from differing run-to-run substrate conditions. These and other errors will be discussed in the following sections as the experimental results are presented.

## IV. RESULTS AND DISCUSSION

### A. Pressure Head Dependence

In this section experimental results of the dependence of the transfer rate on level difference, or pressure head, are presented and discussed. This dependence has already been mentioned in the previous sections regarding the curvature of the  $z(t)$  curves in Figure 5. The critical velocity is observed to respond to pressure, causing the transfer rate to decrease by about 10% over a change in head of 1 1/2 cm in these experiments.

As was discussed in Section II-C in reference to Equation 49, the dependence of the frictional pressure,  $P_g$ , on  $\sigma$  or  $v_g$  can be measured directly when the driving pressure,  $\rho g z$ , is larger than the acceleration term,  $M^* d^2 z/dt^2$ . Figure 7 shows the dependence of  $\sigma$  on  $z$  for three of five beaker fillings during the same experimental run. These curves were obtained by differentiating the same  $z(t)$  curves that were shown in Figure 5. Measurements of the acceleration,  $d^2 z/dt^2$ , made from experimental  $\sigma(z)$  curves such as those shown in Figure 7 indicate that for  $z > 0.01$  cm the acceleration is small enough that the frictional pressure,  $P_g$ , can be set equal to the driving pressure,  $\rho g z$ .

For  $z > 0.1$  cm, the  $\sigma(z)$  data may be described by <sup>54</sup>

$$\sigma(z) = 1/[A - B \ln z(\text{cm})]. \quad (54)$$

Curves of this functional form with A and B as adjustable parameters



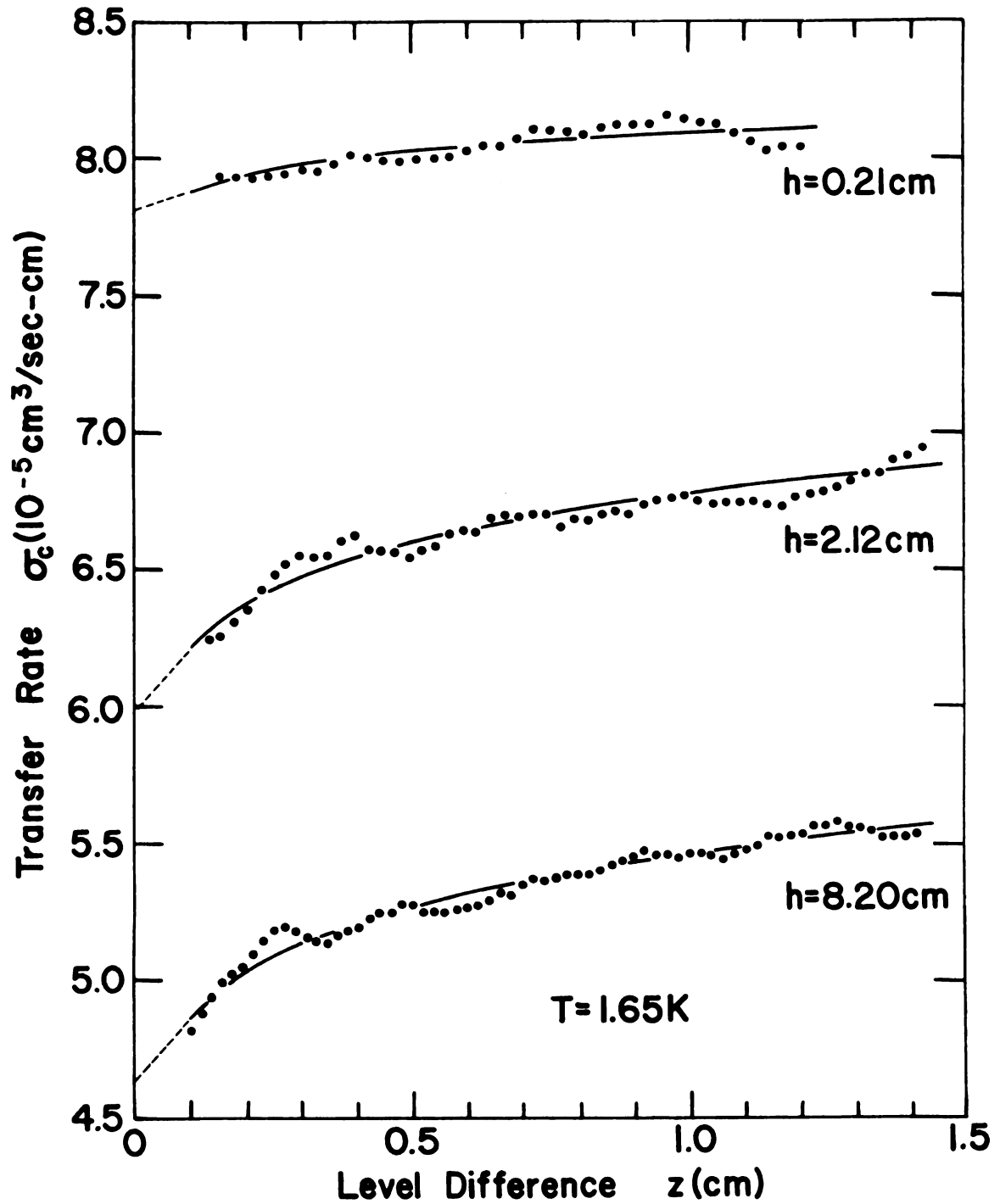


Figure 7: Transfer rate as a function of level difference for the three beaker fillings of Figure 5.

are shown as solid lines on Figure 7. This functional form is a good fit to all the  $\sigma(z)$  data observed in 80 beaker fillings during the clean glass substrate study and also for 35 beaker fillings during the neon substrate study.

The curves in Figure 7 can be interpreted as giving the I-V characteristic of the film. Alternatively, Equation 54 can be inverted to give the dependence of the frictional pressure on  $\sigma$  or  $v_s$ :

$$P_s = \rho g z = C \exp(-1/B\sigma), \quad (55)$$

where C is a constant equal to  $\rho g \exp(A/B)$ . The frictional pressure will have the same functional form using  $v_s$  instead of  $\sigma$ . This is obtained by substituting for  $\sigma$  in Equation 55 using the relation:

$$\sigma = (\rho_s/\rho) v_s d. \quad (56)$$

If  $1/\sigma$  is plotted versus  $\ln z(\text{cm})$  we get a straight line of slope  $-B$  and intercept  $A$  at  $\ln z(\text{cm}) = 0$ . The parameters  $A$  and  $B$  were obtained by fitting the linearized data with a least squared straight line in the computer program Sigma-z. Values of  $A$  and  $B$  are given in the first line of the computer output such as in the output shown in Table A3.

Graphs were drawn after each run  $\sigma$  versus  $z$  and  $1/\sigma$  versus  $\ln z(\text{cm})$  along with the fitted curves to visually check the parameters and goodness of the fit. The data points on these graphs were plotted and the fitted curves were drawn from the computer output using a Hewlett-Packard 9100A calculator and 9125A Calculator Plotter.

Values of the parameters  $A$  and  $B$  were obtained at two temperatures during the clean glass substrate study. At 1.65 K, the values of these parameters are:  $A = (1.80 \pm 0.09) \times 10^4 \text{ sec/cm}^2$  and

$B = (8.9 \pm 1.9) \times 10^2 \text{ sec/cm}^2$  with  $h = 7 \text{ cm}$ . At  $T = 1.28 \text{ K}$ , the values of these parameters are:  $A = (1.35 \pm 0.02) \times 10^4 \text{ sec/cm}^2$  and  $B = (8.3 \pm 1.4) \times 10^2 \text{ sec/cm}^2$  with  $h = 7 \text{ cm}$ . The errors given here are the root mean square deviations of the measured  $A$ 's and  $B$ 's for  $h$  in the neighborhood of  $7 \text{ cm}$ . These errors will be discussed in more detail later in this section. These and other parameters measured during the clean glass and neon substrate studies are presented in tabular form in Appendix B.

For  $z < 0.1 \text{ cm}$ , the acceleration term in the equation of motion becomes important so that the frictional pressure cannot be measured directly. If this term was not included and the fitted curve for large  $z$  was extended to small  $z$ , we would have  $\sigma \rightarrow 0$  as  $z \rightarrow 0$ . However, the acceleration term causes the inner level to overshoot the outer level with  $\sigma \neq 0$  at  $z = 0$ . As was discussed in Section II-C, the inner level then oscillates about the outer level.

The critical velocity, or critical transfer rate, is defined to occur at the velocity where frictional dissipation first occurs. In this experiment the velocity could not be increased from zero until this velocity is reached, as one would like to do. Instead the critical velocity was approached from above with the resulting dynamical limitations. To estimate the zero pressure head or critical transfer rate, a linear extrapolation is made from the fitted curve for large  $z$ . The dashed lines in Figure 7 are such linear extrapolations. Extrapolating from  $z = 0.1 \text{ cm}$ , using  $d\sigma/dz$  evaluated at  $z = 0.1 \text{ cm}$ , we find the following estimate of the zero pressure head transfer rate:

$$\sigma_c = \sigma(0.1 \text{ cm}) - B[\sigma(0.1 \text{ cm})]^2. \quad (57)$$

Here  $\sigma_c$  is taken to be the critical transfer rate of the beaker filling at that  $h$ .

The parameter  $B$  is observed to be independent of  $h$  for  $h > 4$  cm. For  $h < 4$  cm,  $B$  decreases so that  $\sigma$  is nearly independent of  $z$ , as can be seen on the top curve of Figure 7. This decrease of  $B$  at small  $h$  may not be a property of the helium but may be a result of a rapidly changing film thickness when the level difference,  $z$ , is comparable to the height,  $h$ , to the beaker rim. However for  $h=7$  cm, the thickness changes sufficiently slowly with  $h$  that pure pressure head dependence can be seen. Most of the height dependence of  $\sigma$ , which is the subject of the next section, is contained in the parameter  $A$ .

Abrupt changes in the transfer rate from one constant value to another have been reported by Harris-Lowe *et al.*<sup>55</sup> and Allen and Armitage.<sup>48</sup> In this thesis, behavior of the transfer rate has also been seen which is suggestive of these abrupt changes. As the level difference decays, it appears that the data shown in Figures 6 and 7 have a stepped structure as reflected in the departure of the data from the fitted curves.

These deviations of the  $\sigma(z)$  data from the fitted curves are larger than would be expected from the measurement errors of the individual  $\sigma(z)$  points. As was calculated in Section III-D, the average random error in one  $\sigma(z)$  datum point is  $\pm 0.6\%$ . The average rms deviation of the  $\sigma(z)$  points from the fitted curves is, however, found to be  $1.2\%$ . This is twice the deviation that is expected from the measurements. However, more quantitative information about these steps cannot be given because of the low signal-to-noise ratio.

The errors given earlier in this section with the values of the parameters A and B are the rms deviations of the measured A's and B's from their average value for data in the neighborhood of  $h = 7$  cm. These random errors are primarily a result of the deviations on the  $\sigma(z)$  curves. However, the actual errors in the observed A's and B's are slightly greater than would be expected from the  $z(t)$  data because of additional run-to-run deviations arising from differing substrate conditions. The magnitude of  $\sigma$  is primarily determined by the parameter A. The approximately 4% error in A in this experiment is lower than the 10% run-to-run background deviation in  $\sigma$  which was reported by Smith and Boorse.<sup>17</sup>

These  $\sigma(z)$  results are in qualitative agreement with Atkins's<sup>14</sup> original results and with recent results of Martin and Mendelssohn.<sup>56</sup> Similar results were also obtained by Keller and Hammel<sup>57</sup> for flow through a narrow slit.

The functional form of the pressure head dependence agrees with Notarys's<sup>28</sup> observations of superfluid flowing through narrow pores and with his extension of the Langer-Fisher<sup>26</sup> thermal activation theory. However, when this theory is extended to the experiments of this thesis on He film transfer, there are several disagreements with the dependence on other quantities.

The most serious disagreement of these experiments with the Langer-Fisher<sup>26</sup> theory is in the temperature dependence of the parameters A and B. An extension of the Langer-Fisher theory gives  $A(T), B(T) \propto T/(\rho_g/\rho)^2$ . The temperature dependences of the experimental parameters are:  $A(1.65 \text{ K})/A(1.28 \text{ K}) = 1.33$  and  $B(1.65 \text{ K})/B(1.28 \text{ K}) = 1.1$ , while the Langer-Fisher theory predicts

a ratio 1.84 for both A and B. This gives, for the narrow temperature range investigated, a nearly temperature independent B and  $A(T) \propto \rho/\rho_g$ . Hence, within experimental uncertainties we have the usually accepted temperature dependence of  $\sigma_c$ :<sup>1-7</sup>  $\sigma_c \propto \rho_g/\rho$ .

These observed temperature dependences of A and B give an increasing  $d\sigma/dz$  with decreasing temperature in qualitative agreement with the results of Martin and Mendelssohn.<sup>56</sup> As suggested by Martin and Mendelssohn, the increased curvature at lower temperatures may explain the anomalously increasing  $\sigma$ 's with decreasing temperature for  $T < 1$  K that were reported by some experimenters.<sup>1-7</sup>

The functional form of the dependence of the frictional pressure on superfluid velocity observed in these experiments, and also by Notarys,<sup>28</sup> may be true for lower velocities, and pressures, than the limited range investigated in these experiments. If this is true for very small velocities, this would mean that there is no "critical" velocity. That is, for every superfluid velocity, no matter how small, there would be a small frictional pressure. For dynamical reasons, discussed earlier, this could not be tested in this thesis.

Although the Langer-Fisher<sup>26</sup> thermal activation theory does not appear to apply to this experiment, it may be valid for temperatures near  $T_\lambda$ . As was discussed in Section II-C, there may be two competing processes for nucleating vortices. It is possible that a mechanism such as the vortex mill model proposed by Glaberson and Donnelly<sup>23</sup> may dominate at low temperatures while thermal activation dominates at higher temperatures. In this case, the transition temperature from one region to the other would depend on the number of pieces of vortex lines present in the liquid helium. This could explain why Notarys<sup>28</sup> observed the thermal activation

temperature dependence for temperatures down to 1 K while it was not observed in these experiments.

### B. Height Dependence

The critical velocity occurs at the region near the rim of the beaker where the film has its minimum cross sectional area and the velocity is a maximum.<sup>58</sup> Using the dependence of the film thickness on height, the dependence of the critical velocity on film thickness can be determined from measurements of the dependence of  $\sigma$  on the height,  $h$ , of the beaker rim above the reservoir. To do this, we assume that the thickness,  $d$ , of the film at the beaker rim is given by

$$d = k/h^{1/3}, \quad (58)$$

as was calculated in Section II-B for liquid helium adsorbed on a semi-infinite wall.

The critical velocity is expected to have the empirical dependence on film thickness,  $v_c \propto d^{1/4}$ , as was proposed by Van Alphen *et al.*<sup>21</sup> Using Equation 58, this gives  $\sigma_c \propto h^{-1/4}$ . However there is a question concerning which height to use in this relation because the distance to the beaker rim from the bulk liquid is different for the inner and outer levels. Atkins<sup>14</sup> originally suggested that the proper height to use was the height to the beaker rim from the source liquid. This is the distance,  $h$  which is shown in Figure 2, from the beaker rim to the outer level for this experiment. This height was used as a first approximation for the preliminary data analysis.

The dependence of the critical, or zero pressure head, transfer rate,  $\sigma_c$ , on  $h$  is determined from a log-log plot of  $\sigma_c$  versus  $h$ .

Figure 8 shows a log-log plot of  $\sigma_c$  versus  $h$  for the clean glass substrate data at 1.65 K. For  $h > 2$  cm, the data are described by a straight line. A least squares fit to the data for  $h$  in the range 2 cm to 8 cm gives  $\sigma_c = h^{-0.19}$ .<sup>59</sup> For  $h < 2$  cm, the transfer rate is nearly independent of  $h$  as well as  $z$ .

The observations of Figure 8 indicate that the film thickness at the beaker rim is not exactly determined by the height,  $h$ , from the outside, or source, level and that further corrections must be made. Another possible distance that could be used to determine the film thickness is the instantaneous distance to the inner level from the beaker rim. In this case, the film thickness would increase with decreasing  $z$  as the beaker is filling. As a result, when  $h$  is comparable to  $z$ ,  $\sigma$  should increase with decreasing  $z$  as the beaker fills. As can be seen on the top curve of  $\sigma(z)$  in Figure 7, this is not observed.

The data suggest a third possibility. It appears that the data in Figure 8 are displaced by a constant factor in  $h$ . This leads to the plausible assumption that the proper distance to use for determining the film thickness is a distance:

$$h_{\text{corr}} = h + h' > h. \quad (59)$$

This correction appears to be a result of the nonzero initial level difference,  $z_{\text{init}}$ , as suggested by the departure of the data from a straight line in Figure 8 at  $h = 2$  cm, *i.e.*, when  $z_{\text{init}}$  is comparable to  $h$ . This might be similar to metastable behavior that has been seen for beakers that were filled by submersion, *i.e.*, a metastable state of thickness,<sup>60</sup> or vorticity, is formed appropriate to the distance to the beaker rim from the initial inner level.



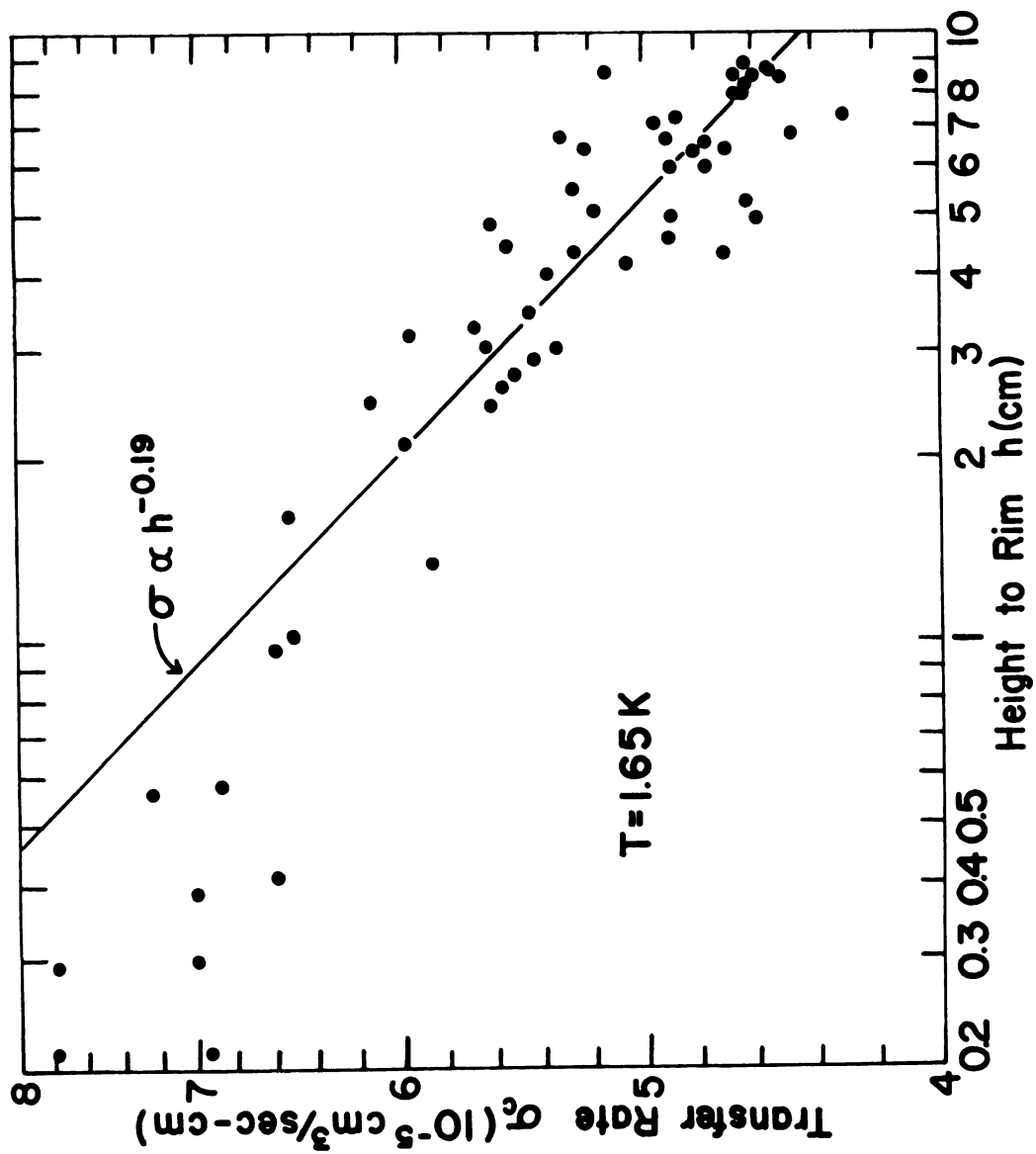


Figure 8: Log-log plot of the critical transfer rate,  $\sigma_c$  with  $T = 1.65 \text{ K}$ , versus height,  $h$ , to the beaker rim.

Other metastable behavior of the film is also suggested by the abrupt changes in the transfer rate, which were mentioned in the previous section.

The above suggestion was tested by performing two experimental runs with a  $z_{\text{init}}$  of 0.3 cm instead of the usual 1 1/2 cm to 2 cm. If the correction is due to  $z_{\text{init}}$ , we would expect that with a smaller  $z_{\text{init}}$  the data would both depart from a straight line at a smaller  $h$  and also have a larger magnitude slope in the straight line region. With  $z_{\text{init}} = 0.3$  cm, the departure of the data from a straight line on the log-log plot appeared to occur at 0.6 cm instead of 2 cm as in the original data. However, the slope of the straight line was  $-0.20$ , essentially the same as the slope for a larger  $z_{\text{init}}$ . Therefore this experimental test was inconclusive and, at worst, may not support the assumption that the correction term  $h'$ , was equal to  $z_{\text{init}}$ .

The following considerations of the quantum mechanical phase,  $\phi$ , make the concept that the thickness at the inside rim of the beaker is determined by the distance to the outside beaker level, plus a possible constant displacement, more palatable.<sup>31</sup> As was discussed in Section II-A, the phase acts as a potential for flow so that on the outside surface of the beaker, where  $v_g$  is subcritical, we have a gradient in  $\phi$ , but  $\phi$  is well defined everywhere in this region. This may again be true along the lower inside surface of the beaker. The dissipative region, where the critical velocity occurs, is near the inside rim of the beaker. In the dissipative region  $\phi$  is not well defined but instead slips at the Josephson frequency. Hence we have a well defined quantum mechanical phase

up the outside surface of the beaker and over the rim up to the dissipative region. This could cause the thickness in the dissipative region to be coupled to the height from the rim to the outside level. However, this does not explain the origin of the displacement,  $h'$ , unless it is possibly due to the finite thickness of the beaker rim.

Nevertheless, if we make the correction,  $h_{\text{corr}} = h + 1 \frac{1}{2} \text{ cm}$ , we not only get a straight line on the log-log plot but also agree with the empirical relation:  $\sigma_c \propto h^{1/4}$ . This is shown in Figure 9. A least squares fit to the corrected 1.65 K data gives:

$$\sigma_c(1.65 \text{ K}) = (8.3 \pm 0.2) h_{\text{corr}}^{-(0.26 \pm 0.05)} \times 10^{-5} \text{ cm}^3/\text{sec-cm}. \quad (60)$$

The error given here for the magnitude of  $\sigma_c$  is the rms scatter of the data from the fitted curve. The error of the exponent was estimated by taking the difference in the slopes of two lines on the log-log plot whose end points differed by twice the rms scatter.

Although we have less data at 1.28 K, if these data are treated in the same way we get:

$$\sigma_c(1.28 \text{ K}) = (10) h_{\text{corr}}^{-1/4} \times 10^{-5} \text{ cm}^3/\text{sec-cm}. \quad (61)$$

These two results are now combined by removing the temperature dependence of  $\sigma$ :

$$\sigma_c(h, T) = (10) (\rho_s/\rho) h_{\text{corr}}^{-1/4} \times 10^{-5} \text{ cm}^3/\text{sec-cm}. \quad (62)$$

Using the dependence of the film thickness on height given in Equation 58, we get the functional dependence of  $v_c$  on  $d$ :  $v_c \propto d^{-1/4}$ . This agrees with the empirical relation of Van Alphen *et al.*<sup>21</sup> This empirical relation was proposed from the examination of several different experiments spanning several decades of channel width of which data the helium film critical velocity formed

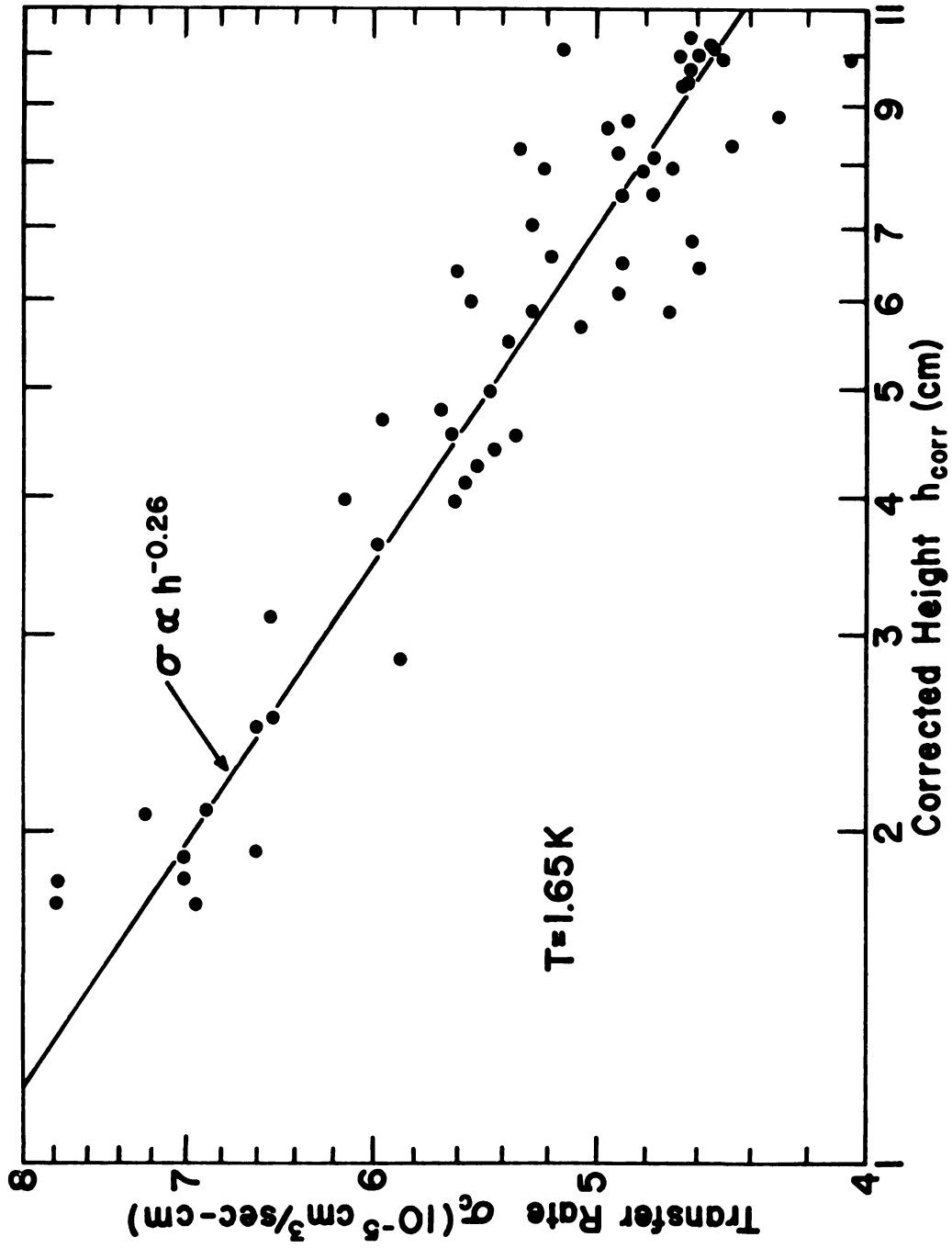


Figure 9: Log-log plot of the critical transfer rate,  $\sigma_c$  with

$T = 1.65 \text{ K}$ , versus corrected height,  $h_{\text{corr}} = h + 1 \frac{1}{2} \text{ cm}$ .

only one point. In the present experiment, this empirical relation was verified over the narrow range of thicknesses covered by the film. This verifies that the proposed dependence is valid for this narrow range. This indicates that the mechanism responsible for the critical velocity in the film is probably the same as for the larger channels.

The dependence,  $v_c d \propto lnd$ , predicted by many theories that use Feynman- Onsager vortices is not observed.<sup>1-7</sup> This does not necessarily disprove these theories but may be a result of a lack of knowledge of how the vortices interact with the channel walls and how they are nucleated.

This functional form of the dependence of  $\sigma$  on  $h$  agrees with the experimental results of Allen and Armitage<sup>48</sup> for the film. Their measurements were made primarily for beaker emptying experiments and were reported at about the same time as these these experiments were begun. The magnitude of  $\sigma_c$  with  $h = 2$  cm agrees with many other experiments<sup>1-7</sup> although it is larger than the results of Allen and Armitage.<sup>48</sup> Van Alphen *et al.* predict  $v_c = ld^{-1/4}$  (c.g.s.).<sup>21</sup> If we use the value  $d = 3.0h^{-1/3} \times 10^{-6}$  cm for the film thickness,<sup>16</sup> Equation 62 gives  $v_c = 1.4d^{-1/4}$  (c.g.s.).

### C. Substrate Dependence

Results are reported and discussed in this section of measurements of the transfer rate on a neon substrate. As was discussed in Section III-B, an effective neon substrate was prepared by coating a clean glass beaker with neon taking care to provide smooth and uniform surface conditions. Using this method, a decrease in  $\sigma$

was seen going from a clean glass substrate to an effective neon substrate in the same apparatus.

Using the results of the previous two sections, the dependences of  $\sigma$  on  $h$  and  $z$  could be separated and the substrate dependence isolated. During an experimental run with a neon substrate, measurements were made of  $z(t)$  at three  $h$ 's: typically at  $h = 5$  cm, 7 cm and 9 cm. The  $\sigma(z)$  curves were then determined and the  $z$  dependence of the data removed by using the zero pressure head transfer rate,  $\sigma_c$ . The dependence of  $\sigma_c$  on  $h$  was then removed from  $\sigma_c$  by normalizing the data to  $h = 7$  cm using the dependence :

$$\sigma_c \propto h^{-1/4}.$$

During the neon substrate study, three runs were made using only the clean glass beaker without a neon coating. The first clean glass run was made after the final assembly of the apparatus for comparison with the results of the previous sections. Two other clean glass runs were made with the neon substrate apparatus during the course of the neon substrate study as a test of the cleanliness of the beaker. The transfer rates obtained for these runs agree with the previous clean glass substrate results demonstrating that the beaker was initially clean, and remained clean during the course of the substrate study.

All of the data during the neon substrate study were taken at a temperature of 1.65 K, as were most of the clean glass substrate data of the previous sections. Transfer rates for a neon substrate were determined as a function of the thickness of the neon coating,  $\xi$ . Figure 10 shows  $\sigma_c$  with  $h = 7$  cm and  $T = 1.65$  K as a function of  $\xi$ . The three points at the left of this figure are the clean

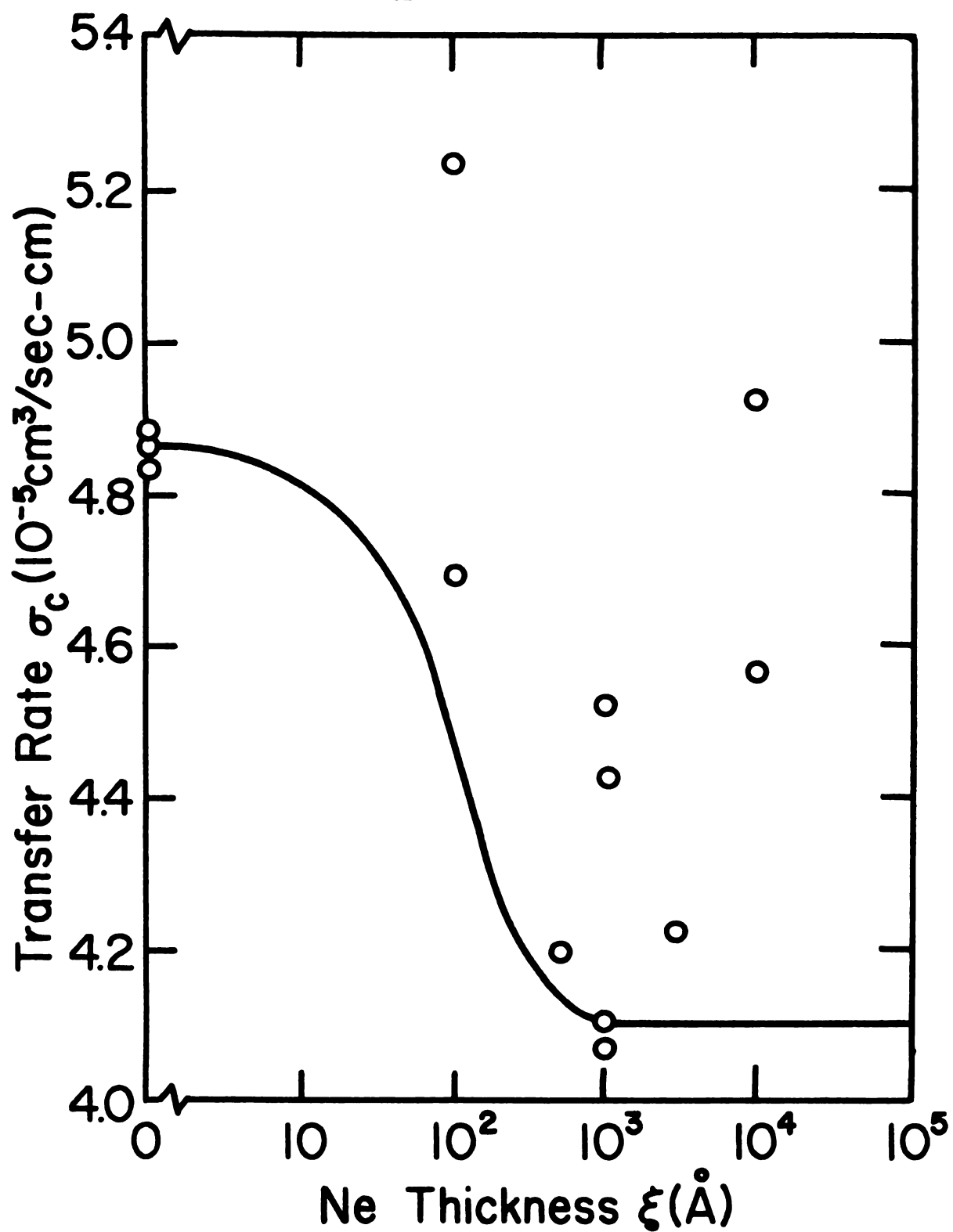


Figure 10: Semi-log plot of the critical transfer rate,  $\sigma_c$  with  $h=7\text{cm}$  and  $T = 1.65 \text{ K}$ , versus thickness of Ne coating,  $\xi$ .

glass substrate transfer rates obtained with this apparatus.

The  $\sigma(\xi)$  results shown on Figure 10 are more meaningful than seems upon initial inspection. For a neon coating of about  $1000 \text{ \AA}$ , it was possible to see an on-off effect; i.e., the substrate could be changed relatively reproducibly from clean glass to neon at will. Because of the logarithmic neon thickness scale, the larger than expected transfer rates at very high and very low coverages make the  $\sigma(\xi)$  data look worse than they really are. Although some of the transfer rates are larger than expected, all of the neon substrate transfer rates for  $\xi > 500 \text{ \AA}$  are, however, less than the clean glass transfer rates.

The lowest transfer rates were seen over the decade of neon thickness from  $500 \text{ \AA}$  to  $5000 \text{ \AA}$ . Four experimental runs having a neon coating in this thickness range gave a critical transfer rate of  $\sigma_c(h=7 \text{ cm}) = 4.1 \times 10^{-5} \text{ cm}^3/\text{sec-cm}$ . Two other runs at  $1000 \text{ \AA}$  thickness neon coating gave  $\sigma_c = 4.4 \times 10^{-5} \text{ cm}^3/\text{sec-cm}$ . These larger transfer rates are most likely a result of accidentally rough neon coatings. For comparison, the average clean glass transfer rate in this apparatus was:  $\sigma_c = 4.86 \times 10^{-5} \text{ cm}^3/\text{sec-cm}$ .

At  $100 \text{ \AA}$  thickness neon coating, we expect to have a helium film thickness equal to the average of the film thicknesses on clean glass and pure neon substrates. Two measurements were made of  $\sigma_c$  at this neon coverage. One of these experiments gave  $\sigma_c = 4.7 \times 10^{-5} \text{ cm}^3/\text{sec-cm}$ , approximately as expected. The other experiment, probably due to rough substrate conditions, gave the larger transfer rate:  $\sigma_c = 5.2 \times 10^{-5} \text{ cm}^3/\text{sec-cm}$ .

At  $10\,000 \text{ \AA}$  thickness neon coverage, larger transfer rates



than the minimum are again seen. From the calculated helium film thickness as a function of  $\xi$ , this is not expected. Two measurements were made of  $\sigma_c$  at this coverage. These transfer rates had an average value of  $\sigma_c = 4.7 \times 10^{-5} \text{ cm}^3/\text{sec-cm}$ . At this large thickness, it may not be possible to get a smooth neon coating using the method described in Section III-B. Because of the long annealing times used in this procedure to smooth the neon coating, it may be that a granular layer is formed as a result of crystallization of the thick neon coating.

The functional form of the expected dependence of  $\sigma_c$  on film thickness can be calculated using the results of the previous sections:  $\sigma_c = v_c d$  and  $v_c = d^{-1/4}$ . These results give  $\sigma_c = d^{3/4}$ . Using this dependence, the expected dependence of  $\sigma_c$  on the thickness of the neon coating,  $\xi$ , can be determined from the plot of the helium film thickness versus  $\xi$  shown in Figure 1. This expected functional dependence is shown as the solid curve on Figure 10. This curve has been normalized to go through the experimental clean glass substrate points and the lowest 1000 Å thickness neon coating points which have average transfer rates of  $4.86 \times 10^{-5} \text{ cm}^3/\text{sec-cm}$  and  $4.1 \times 10^{-5} \text{ cm}^3/\text{sec-cm}$  respectively.

The ratio of the thickness of the helium film on the effective neon substrate to the thickness of the helium film on the clean glass substrate is now calculated from the experimental results. Using the lowest neon substrate transfer rate and the clean glass substrate transfer rate, given above, we get

$$d_{\text{Ne}}/d_{\text{glass}} = (\sigma_{\text{Ne}}/\sigma_{\text{glass}})^{4/3} = 0.79. \quad (63)$$

Assuming the film thickness,  $d_{\text{glass}} = 3.0h^{-1/3} \times 10^{-6}$  cm, for a clean glass substrate,<sup>43</sup> the thickness of the helium film on a neon substrate can be calculated using Equation 63. Solving this equation, we get  $d_{\text{Ne}} = 2.4h^{-1/3} \times 10^{-6}$  cm. This experimental value of the film thickness agrees remarkably well with the result:

$d_{\text{Ne}} = 2.3h^{-1/3} \times 10^{-6}$  previously calculated in Section II-B.

## V. SUMMARY AND CONCLUSIONS

Measurements of helium film transfer rates for filling clean glass and neon coated beakers have been reported in the previous sections. The apparatus used in this study was designed to provide a clean environment for the beaker, to avoid enhanced transfer rates and unnecessary background variations. With this apparatus, quantitative measurements could be made of the slight dependences of the transfer rate,  $\sigma$ , on pressure head, film height, and substrate material.

The pressure head dependence of  $\sigma$  was measured over a change in head,  $z$ , from 2 cm to 0.1 cm. The data in this range are described by the functional dependence:

$$\sigma(z) = 1/[A - B \ln(z)]. \quad (64)$$

This gives a dependence on superfluid velocity,  $v_s$ , of the frictional pressure,  $P_s$ , opposing the flow of  $P_s = \exp[f(h,T)/v_s]$ . These results agree with previous, qualitative measurements by other experimenters of the pressure head dependence for both the film and narrow channels.

The dependence of the critical, or zero pressure head, transfer rate,  $\sigma_c$ , on the height,  $h$ , of the beaker rim above the outer helium level was measured for  $h$  ranging from a few millimeters to 10 cm. After applying corrections, which were discussed in Section IV-B, these data are described by:

$$\sigma_c(h_{\text{corr}}) = \sigma_o h_{\text{corr}}^{-1/4}, \quad (65)$$

where  $\sigma_0$  is a constant for a given temperature and  $h_{\text{corr}}$  is the corrected height. This results in the dependence,  $v_c \propto d^{-1/4}$ , of the critical velocity,  $v_c$ , on channel width,  $d$ . This dependence agrees with recent measurements by Allen and Armitage<sup>48</sup> for the film and the empirical relation proposed by Van Alphen *et al.*<sup>21</sup>

A 16% decrease was seen in the transfer rate going from a clean glass substrate to an effective neon substrate in the same apparatus. The helium film thickness on a neon substrate, derived from this change in  $\sigma$ , is in reasonable agreement with the thicknesses calculated for rare-gas solids in Section II-B.

Although the physical mechanism for the critical velocity is believed to be vortex production, basic theories using this mechanism are not sufficiently well developed to predict these measured dependences on pressure head and film height. We hope these results can be used as a guide in the solution of these problems.

## **LIST OF REFERENCES**

## LIST OF REFERENCES

1. K. R. Atkins, *Liquid Helium* (Cambridge University Press, Cambridge, England, 1959).
2. R. J. Donnelly, *Experimental Superfluidity* (University of Chicago Press, Chicago, 1967).
3. J. G. Daunt and R. S. Smith, *Rev. Mod. Phys.* 26, 172 (1954).
4. L. C. Jackson and L. G. Grimes, *Phil. Mag. Suppl.* 7, 435 (1958).
5. W. E. Kaller, *Helium-3 and Helium-4* (Plenum Press, New York, 1969).
6. C. T. Lane, *Superfluid Physics* (McGraw-Hill, New York, 1962).
7. J. Wilks, *Liquid and Solid Helium* (Clarendon Press, Oxford, England, 1967).
8. W. H. Keesom, *Helium* (Elsevier, Amsterdam, 1942).
9. L. Tisza, *Nature* 141, 913 (1938); *Compt. Rend.* 207, 1035, 1186 (1938); *J. Phys. Radium* 1, 165, 350 (1941); *Phys. Rev.* 72, 838 (1947); and *Phys. Rev.* 75, 885 (1949).
10. F. London, *Superfluids, Vol. II* (Wiley, New York, 1954).
11. L. Landau, *Phys. Rev.* 60, 357 (1941); *J. Phys. (U.S.S.R.)* 5, 71 (1941); *J. Phys. (U.S.S.R.)* 8, 1 (1944); *J. Phys. (U.S.S.R.)* 11, 91 (1947); and *Phys. Rev.* 75, 884 (1949).
12. B. V. Rollin and F. Simon, *Physica* 6, 219 (1939).
13. J. G. Daunt and K. Mendelssohn, *Proc. Roy. Soc. (London)* A170, 423 (1939); A170, 439 (1939).
14. K. R. Atkins, *Proc. Roy. Soc. (London)* A203, 240 (1950).
15. B. N. Esel'son and B. G. Lazarev, *Zh. Eksp. Teor. Fiz.* 23, 552 (1952).
16. P. W. F. Gribbon and L. C. Jackson, *Can. J. Phys.* 41, 1047 (1963).
17. B. Smith and H. A. Boorse, *Phys. Rev.* 98, 328 (1955); 99, 346 (1955); 99, 358 (1955); 99, 367 (1955).

18. L. Onsager, *Nuovo Cimento Suppl.* 6, 2249 (1949).
19. R. P. Feynman, in *Progress in Low Temperature Physics, Vol. I*, edited by C. J. Gorter (North Holland, Amsterdam, 1955), p. 17.
20. Ref. 5, Chapter 8.
21. W. M. Van Alphen, G. J. Van Haasteren, R. DeBruyn Ouboter, and K. W. Taconis, *Phys. Letters* 20, 474 (1966).
22. W. F. Vinen, in *Progress in Low Temperature Physics, Vol. III*, edited by C. J. Gorter (North Holland, Amsterdam, 1955), p. 1; in *Liquid Helium*, edited by G. Careri (Academic Press, New York, 1963), p. 336; and in *Quantum Fluids*, edited by D. F. Brewer (North Holland, Amsterdam, 1966), p. 74.
23. W. I. Glaberson and R. J. Donnelly, *Phys. Rev.* 141, 208 (1966).
24. V. P. Peshkov, in *Proceedings of the VII International Conference on Low Temperature Physics*, edited by G. M. Graham and A. C. H. Hallett (University of Toronto Press, Toronto, 1961), p. 555; in *Progress in Low Temperature Physics, Vol. IV*, edited by C. J. Gorter (North Holland, Amsterdam, 1966), p. 1.
25. P. P. Craig, *Phys. Letters* 21, 385 (1966).
26. J. S. Langer and M. E. Fisher, *Phys. Rev. Letters* 19, 560 (1967); M. E. Fisher, in *Proceedings of the International Conference on Fluctuations in Superconductors*, edited by W. S. Goree and F. Chilton (Stanford Research Institute, Menlo Park, Calif., 1968), p. 357.
27. J. R. Clow and J. D. Reppy, *Phys. Rev. Letters* 19, 91 (1967).
28. H. A. Notarys, *Phys. Rev. Letters* 22, 1240 (1969).
29. S. T. Beliaev, *Soviet Phys.—JETP* 7, 289 (1969).
30. P. W. Anderson, *Rev. Mod. Phys.* 38, 298 (1966); also in *Quantum Fluids*, edited by D. F. Brewer (North Holland, Amsterdam, 1966), p. 146.
31. R. J. Donnelly, *Phys. Rev. Letters* 14, 939 (1965).
32. L. I. Schiff, *Phys. Rev.* 59, 839 (1941).
33. T. L. Hill, *Advances in Catalysis and Related Subjects, Vol. IV* (Academic Press, New York, 1952), p. 211.
34. G. L. Pollack, *Rev. Mod. Phys.* 36, 748 (1964).
35. G. K. Horton, *Am. J. Phys.* 36, 93 (1968).

36. J. W. Rowlinson and J. R. Townly, *Trans. Faraday Soc.* 49, 20 (1953).
37. I. E. Dzyaloshinskii, E. M. Lifshitz, and L. P. Pitaevskii, *Soviet Phys.—JETP* 10, 161 (1960); *Advan. Phys.* 10, 165 (1961).
38. V. M. Kontorovich, *Soviet Phys.—JETP* 3, 770 (1956).
39. W. E. Keller, *Phys. Rev. Letters* 24, 569 (1970).
40. D. L. Goodstein and P. G. Saffman, *Phys. Rev. Letters* 24, 1402 (1970).
41. R. Bowers, *Phil. Mag.* 44, 465 (1953); 44, 485 (1953).
42. K. R. Atkins, *Proc. Roy. Soc. (London)* 203A, 119 (1950).
43. A. C. Ham and L. C. Jackson, *Proc. Roy. Soc. (London)* A240, 243 (1957).
44. K. R. Atkins, *Nature* 161, 925 (1948).
45. W. J. de Haas and G. J. van den Berg, *Rev. Mod. Phys.* 76, 609 (1949).
46. R. Bowers and K. Mendelssohn, *Proc. Phys. Soc. (London)* 63A, 1318 (1950).
47. N. G. McCrum and J. C. Eisenstein, *Phys. Rev.* 99, 1326 (1955).
48. J. F. Allen and J. G. M. Armitage, *Phys. Letters* 22, 121 (1966).
49. G. S. Picus, *Phys. Rev.* 94, 1459 (1954).
50. J. N. Schubb and I. E. Pollard, *La Vide* 23, 64 (1969).
51. J. G. Dash, *Phys. Rev.* A1, 7 (1970).
52. G. K. White, *Experimental Techniques in Low-Temperature Physics* (Clarendon Press, Oxford, England, 1959), p. 115.
53. C. Mack, *Essentials of Statistics for Scientists and Technologists* (Plenum Press, New York, 1967).
54. C. J. Duthler and G. L. Pollack, *Phys. Letters* 31A, 390 (1970).
55. R. F. Harris-Lowe, C. F. Mate, K. L. McCloud, and J. G. Daunt, *Phys. Letters* 20, 126 (1966).
56. D. J. Martin and K. Mendelssohn, *Phys. Letters* 30A, 107 (1969).
57. W. E. Keller and E. F. Hammel, *Physics* 2, 221 (1966).
58. W. E. Keller and E. F. Hammel, *Phys. Rev. Letters* 17, 998 (1966).



59. C. J. Duthler and G. L. Pollack, Bull. Am. Phys. Soc. 13, 912 (1968); 14, 96 (1969).
60. J. F. Allen and C. C. Matheson, Proc. Roy. Soc. (London) A290, 1 (1966).

## **APPENDICES**

## APPENDIX A: COMPUTER PROGRAM FOR DATA REDUCTION

TABLE A1

Fortran listing of the computer program, Sigma-z, used in the  $\sigma(z)$  analysis.

```

01      PROGRAM SIGMA Z (INPUT,OUTPUT)
C      DIMENSION TM(300),H(300),TS(300),Z(300),SIGMA(300),DELTA(300) ,
C      LNZ(300),ASIG(300)
C      INTEGER P,Q,R,S
C      REAL LNZ
C      I=1$P=0$Q=10$R=5
C      READ INPUT DATA
C
C      READ 02,RUN
C      FORMAT (A10)
C      READ 03,H0,G
C      FORMAT (2F6.0)
C      READ 05, TM(I),H(I),TM(I+1),H(I+1),TM(I+2),H(I+2),TM(I+3),H(I+3),
C      1 TM(I+4),H(I+4),TM(I+5),H(I+5),K
C      FORMAT (12F6.0,I1)
C      I=I+6
C      IF (K.EQ.0) GO TO 04
C      READ 07, TM(I),H(I),K
C      FORMAT (2F6.0,I1)
C      I=I+1
C      IF (K.EQ.0) GO TO 06
C
C      CALCULATE DELTA, Z, AND TIME IN SEC
C
C      N=I-1 $DELTA(1)=0.0 $ TS(1)=60.0*TM(1) $Z(1)=H0-H(1)
C      DO 08 I=2,N

```

```

08      DELTA(I)=H(I)-H(I-1)
        TS(I)=60.0*TM(I)
        Z(I)=HO-H(I)
C
C      FIT 11 PT. Z(T) SEGMENTS WITH QUADRATIC, Z(T) = A+BT+CT*2
C      EVALUATE SIGMA AT MIDPOINT OF SEGMENT
C
09      P=P+1 $ Q=Q+1 $ ST=0.0 $ ST2=0.0 $ ST3=0.0 $ ST4=0.0
        SZ=0.0 $ STZ=0.0 $ ST2Z=0.0
        DO 10 I=P,Q
          ST=ST+TS(I) $ ST2=ST2+TS(I)**2
          ST3=ST3+TS(I)**3 $ ST4=ST4+TS(I)**4
          SZ=SZ+Z(I) $ STZ=STZ+TS(I)*Z(I)
          ST2Z=ST2Z+Z(I)*TS(I)**2
        10      CONTINUE
        D=11.0*ST2*ST4-11.0*ST3**2-(ST**2)*ST4+2.0*ST*ST2*ST3-ST2**3
        DA=SZ*ST2*ST4-SZ*ST3**2-STZ*ST*ST4+ST2Z*ST*ST3+ST2*ST2*ST3
        1-ST2Z*ST2**2
        DB=11.0*STZ*ST4-11.0*ST2Z*ST3-SZ*ST*ST4+SZ*ST2*ST3+ST2Z*ST*ST2
        1-STZ*ST2**2
        DC=11.0*ST2Z*ST2-11.0*STZ*ST3-ST2Z*ST**2+STZ*ST*ST2+SZ*ST*ST3
        1-SZ*ST2**2
        A=DA/D $ B=DB/D $ C=DC/D $ R=R+1
        SIGMA(R)=G*SQRT(B**2-4.0*C*(A-Z(R)))
        IF (Q.LT.N) GO TO 09
C
C      DEFINE UNCALCULATED PTS. TO BE ZERO
C
        DO 11 R=1,5
          LNZ(R)=0.0 $ ASIG(R)=0.0
          SIGMA(R)=0.0
          S=N-4
        11
        DO 12 R=S,N
          LNZ(R)=0.0 $ ASIG(R)=0.0
          SIGMA(R)=0.0
          S=N-5
        12

```

```

C      CALCULATE 1/SIGMA AND LN(Z)
C
C      DO 13 I=6,S
C      LNZ(I)=ALOG(Z(I))
C      ASIG(I)=1.0/SIGMA(I)
C
C      FIT      SIGMA = 1/(A-B*LN(Z))
C
C      N1=N-10 $ N2=N-5 $ SLN=0.0 $ SLN2=0.0 $ SAS=0.0 $ SASL=0.0
C      DO 18 I=6,N2
C      SLN=SLN + LNZ(I) $ SLN2= SLN2 + (LNZ(I))**2
C      SAS=SAS + ASIG(I) $ SASL=SASL + ASIG(I)*LNZ(I)
C      CONTINUE
C      D1=N1*SLN2-SLN**2
C      DA1=SAS*SLN2-SLN*SASL
C      DB1=N1*SASL-SLN*SAS
C      A1=DA1/D1 $ B1=-DB1/D1
C
C      PRINT OUTPUT
C
C      PRINT 14,RUN,H0,G,A1,B1
C      FORMAT (1H1,6X,4HRUN ,A4,6X,4HH0= ,F6.3,6X,3HG= ,F6.0,6X,3HA= ,
C      11PE10.3,6X,3HB= ,1PE9.2 ///)
C      PRINT 15
C      FORMAT (14X,1HN,11X,5HT MIN,12X,1HH,12X,5HDELTA,12X,1HZ,12X,
C      15HSIGMA,11X,4HLN Z,8X,7H1/SIGMA //)
C      N=N+1 $ I=1
C      PRINT 17,I,TM(I),H(I),DELTA(I),Z(I),SIGMA(I),LNZ(I),ASIG(I)
C      FORMAT (1H ,115,F15.2,5F15.3,F15.5)
C      I=I+1
C      IF (I.LT.N) GO TO 16
C      IF (K.LT.9) GO TO 01
C      END

```

**TABLE A2**  
**Typical input data to computer program for one beaker filling.**

[illegible]

TABLE A3

Computer output for data of Table 2.

RUN 65A	H0= 1.884	G= 8090.	A= 1.830E-01	B= 9.43E-03					
N	T MIN	H	DELTA	Z	SIGMA	LN Z	1/SIGMA		
1	0.00	.417	0.000	1.467	0.000	0.000	0.00000		
2	.50	.439	.022	1.445	0.000	0.000	0.00000		
3	1.00	.458	.019	1.426	0.000	0.000	0.00000		
4	1.50	.479	.021	1.405	0.000	0.000	0.00000		
5	2.00	.499	.020	1.385	0.000	0.000	0.00000		
6	2.50	.519	.020	1.365	5.528	.311	.18090		
7	3.00	.541	.022	1.343	5.527	.295	.18094		
8	3.50	.560	.019	1.324	5.550	.281	.18018		
9	4.00	.581	.021	1.303	5.560	.265	.17986		
10	4.50	.602	.021	1.282	5.567	.248	.17962		
11	5.00	.623	.021	1.261	5.585	.232	.17906		
12	5.50	.643	.020	1.241	5.570	.216	.17954		
13	6.00	.664	.021	1.220	5.568	.199	.17961		
14	6.50	.685	.021	1.199	5.538	.181	.18058		
15	7.00	.705	.020	1.179	5.533	.165	.18073		
16	7.50	.727	.022	1.157	5.525	.146	.18099		
17	8.00	.746	.019	1.138	5.531	.129	.18081		
18	8.50	.766	.020	1.118	5.497	.112	.18192		
19	9.00	.786	.020	1.098	5.480	.093	.18249		
20	9.50	.808	.022	1.076	5.466	.073	.18294		
21	10.00	.828	.020	1.056	5.447	.054	.18359		
22	10.50	.849	.021	1.035	5.461	.034	.18312		
23	11.00	.867	.018	1.017	5.469	.017	.18283		
24	11.50	.888	.021	.996	5.467	-.004	.18292		
25	12.00	.908	.020	.976	5.454	-.024	.18334		
26	12.50	.928	.020	.956	5.462	-.045	.18310		
27	13.00	.949	.021	.935	5.464	-.067	.18300		
28	13.50	.970	.021	.914	5.476	-.090	.18261		
29	14.00	.990	.020	.894	5.457	-.112	.18326		
30	14.50	1.010	.020	.874	5.445	-.135	.18366		

31	15.00	1.030	.020	.854	5.428	-.158	.18424
32	15.50	1.050	.020	.834	5.406	-.182	.18499
33	16.00	1.070	.020	.814	5.393	-.206	.18541
34	16.50	1.090	.020	.794	5.393	-.231	.18541
35	17.00	1.110	.020	.774	5.393	-.256	.18541
36	17.50	1.130	.020	.754	5.381	-.282	.18584
37	18.00	1.150	.020	.734	5.371	-.309	.18617
38	18.50	1.170	.020	.714	5.376	-.337	.18601
39	19.00	1.190	.020	.694	5.356	-.365	.18669
40	19.50	1.210	.020	.674	5.317	-.395	.18807
41	20.00	1.229	.019	.655	5.325	-.423	.18780
42	20.50	1.249	.020	.635	5.298	-.454	.18875
43	21.00	1.270	.021	.614	5.280	-.488	.18941
44	21.50	1.288	.018	.596	5.273	-.518	.18964
45	22.00	1.306	.018	.578	5.264	-.548	.18997
46	22.50	1.329	.023	.555	5.253	-.589	.19038
47	23.00	1.346	.017	.538	5.256	-.620	.19027
48	23.50	1.366	.020	.518	5.256	-.658	.19026
49	24.00	1.386	.020	.498	5.283	-.697	.18928
50	24.50	1.405	.019	.479	5.283	-.736	.18928
51	25.00	1.424	.019	.460	5.253	-.777	.19036
52	25.50	1.445	.021	.439	5.253	-.823	.19037
53	26.00	1.464	.019	.420	5.232	-.868	.19115
54	26.50	1.484	.020	.400	5.199	-.916	.19236
55	27.00	1.503	.019	.381	5.187	-.965	.19279
56	27.50	1.522	.019	.362	5.168	-1.016	.19351
57	28.00	1.540	.018	.344	5.141	-1.067	.19452
58	28.50	1.560	.020	.324	5.148	-1.127	.19423
59	29.00	1.578	.018	.306	5.162	-1.184	.19372
60	29.50	1.598	.020	.286	5.185	-1.252	.19285
61	30.00	1.617	.019	.267	5.202	-1.321	.19223
62	30.50	1.636	.019	.248	5.190	-1.394	.19266
63	31.00	1.656	.020	.228	5.151	-1.478	.19414
64	31.50	1.676	.020	.208	5.100	-1.570	.19607
65	32.00	1.695	.019	.189	5.055	-1.666	.19782
66	32.50	1.714	.019	.170	5.027	-1.772	.19891
67	33.00	1.731	.017	.153	4.997	-1.877	.20013
68	33.50	1.749	.018	.135	4.945	-2.002	.20222
69	34.00	1.766	.017	.118	4.886	-2.137	.20467
70	34.50	1.786	.020	.098	4.822	-2.323	.20737
71	35.00	1.805	.019	.079	0.000	0.000	0.00000
72	35.50	1.823	.018	.061	0.000	0.000	0.00000
73	36.00	1.840	.017	.044	0.000	0.000	0.00000
74	36.50	1.856	.016	.028	0.000	0.000	0.00000
75	37.00	1.872	.016	.012	0.000	0.000	0.00000



# APPENDIX B

## TABULAR TRANSFER RATE DATA

TABLE B1  
Measured transfer rate parameters for a clean glass  
substrate and T = 1.65 K.

Run No.	h (cm)	A ( $10^4 \text{ sec/cm}^2$ )	B ( $10^2 \text{ sec/cm}^2$ )	$\sigma_c$ ( $10^{-5} \text{ cm}^2/\text{sec}$ )
57A	7.897	1.843	9.07	4.658
57B	6.374	1.769	9.21	4.813
57C	4.363	1.676	13.29	4.707
57D	2.758	1.604	6.32	5.509
57E	0.413	1.405	3.29	6.603
58A	8.867	1.788	11.11	4.627
58B	7.233	1.739	9.32	4.875
58C	5.533	1.678	6.57	5.270
58D	3.473	1.612	6.64	5.453
58E	0.974	1.440	2.25	6.602
59A	8.619	1.735	6.32	5.139
59B	6.754	1.667	6.39	5.318
59C	4.879	1.597	5.61	5.605
59D	3.184	1.558	3.61	5.959
59E	0.582	1.385	2.07	6.879
60A	8.387	2.134	10.00	4.051
60B	6.803	2.026	6.36	4.468
60C	4.948	1.847	9.86	4.592
60D	2.910	1.676	4.93	5.434
60E	0.213	1.376	1.93	6.944
61A	8.705	1.865	9.96	4.548
61B	7.093	1.786	6.96	4.954
61C	5.092	1.688	7.18	5.187
61D	3.050	1.591	5.57	5.628
61E	0.565	1.354	0.82	7.240
62A	8.498	1.876	8.93	4.598
62B	6.675	1.770	7.93	4.913
62C	4.996	1.693	10.39	4.897
62D	3.038	1.599	8.14	5.343
62E	1.021	1.421	3.43	6.514
63A	8.646	1.857	10.32	4.539
63B	6.607	1.744	10.50	4.770
63C	4.602	1.648	11.57	4.908
63D	2.615	1.533	7.89	5.564
63E	0.301	1.257	5.07	7.011

Table B1 (cont'd.)

Run	h	A	B	$\sigma_c$
No.	(cm)	( $10^4 \text{ sec/cm}^2$ )	( $10^2 \text{ sec/cm}^2$ )	( $10^{-5} \text{ cm}^2/\text{sec}$ )
64A	7.960	1.863	8.79	4.636
64B	6.008	1.734	10.75	4.773
64C	4.012	1.664	5.89	5.375
64D	1.614	1.426	3.14	6.534
65A	8.197	1.829	9.89	4.628
65B	5.994	1.698	10.25	4.897
65C	4.191	1.616	10.64	5.066
65D	2.122	1.475	5.86	5.985
65E	0.213	1.236	1.46	7.786
66A	8.395	1.914	9.14	4.505
66B	6.427	1.794	9.96	4.699
66C	4.379	1.695	6.11	5.266
66D	2.452	1.555	6.79	5.612
66E	0.389	1.332	2.82	7.014
67A	7.325	2.025	9.04	4.297
67B	5.300	1.792	11.00	4.626
67C	3.289	1.617	4.32	5.679
67D	1.350	1.401	9.00	5.870
68A	8.478	1.777	10.93	4.664
68B	6.423	1.696	6.54	5.224
68C	4.498	1.591	6.43	5.538
68D	2.471	1.472	4.68	6.143
68E	0.294	1.229	1.71	7.778

TABLE B2  
 Measured transfer rate parameters for a clean glass  
 substrate and  $T = 1.28$  K.

Run	h	A	B	$\sigma_c$
No.	(cm)	( $10^4 \text{ sec/cm}^2$ )	( $10^2 \text{ sec/cm}^2$ )	( $10^{-5} \text{ cm}^2/\text{sec}$ )
71A	8.747	1.374	8.14	6.071
71B	6.734	1.330	6.89	6.407
71C	4.761	1.311	9.14	6.178
71D	2.700	1.257	6.71	6.748
71E	0.389	1.100	3.18	8.293
72A	8.410	1.388	8.57	5.967
72B	6.493	1.327	6.43	6.484
72C	4.483	1.283	10.64	6.089
72D	2.474	1.213	7.57	6.815
72E	0.373	1.096	1.46	8.738
73A	8.760	1.399	9.14	5.860
73B	6.894	1.362	7.07	6.254
73C	4.949	1.329	7.14	6.376
73D	2.975	1.274	6.25	6.742
73E	0.911	1.130	2.04	8.349
74A	7.579	1.396	7.46	6.075
74B	5.676	1.283	10.82	6.066
74C	3.681	1.300	9.11	6.224
74D	1.675	1.178	7.75	6.951

TABLE B3

Measured transfer rate data for a neon substrate and  $T = 1.65$  K.

Run	$\xi$	$h$	A	B	$\sigma_c$
No.	( $\text{\AA}$ )	(cm)	( $10^4 \text{ sec/cm}^2$ )	( $10^2 \text{ sec/cm}^2$ )	( $10^{-5} \text{ cm}^2/\text{sec}$ )
77A	0	9.337	1.972	7.56	4.50
77B	0	7.635	1.876	5.72	4.84
77C	0	5.459	1.776	5.39	5.11
78A	1000	9.350	2.344	9.31	3.77
78B	1000	7.517	2.210	6.58	4.12
78C	1000	5.588	2.051	8.39	4.29
78D	1000	3.397	1.870	5.03	4.91
79A	1000	9.120	2.208	7.19	4.09
79B	1000	7.177	2.046	5.94	4.46
80A	1000	9.130	2.373	11.88	3.61
80B	1000	7.142	2.186	8.03	4.08
80C	1000	5.116	2.022	5.02	4.57
81A	0	0.092	1.969	7.53	4.50
81B	0	7.051	1.837	5.60	4.94
82A	10 000	8.908	1.979	5.87	4.60
82B	10 000	6.853	1.832	5.10	5.00
83A	3000	8.991	2.265	9.24	3.89
83B	3000	7.039	2.104	6.70	4.30
84A	500	6.435	2.068	8.02	4.28
85A	100	9.288	2.060	7.43	4.33
85B	100	7.289	1.930	6.54	4.65
85C	100	5.284	1.826	4.44	5.07
86A	10 000	9.126	2.111	8.65	4.17
86B	10 000	7.212	1.991	5.34	4.61
86C	10 000	5.211	1.873	4.49	4.94
87A	100	1.129	1.864	5.22	4.90
87B	100	7.150	1.765	3.62	5.30
87C	100	5.120	1.675	3.64	5.57
88A	0	9.129	1.969	6.52	4.57
88B	0	7.230	1.857	6.26	4.84
88C	0	5.206	1.754	6.47	5.08
89A	1000	9.130	2.167	7.57	4.13
89B	1000	7.089	1.990	6.34	4.54
89C	1000	4.997	1.850	4.79	4.98



MICHIGAN STATE UNIVERSITY LIBRARIES



3 1293 03071 2966